Nuclear Medicine and Molecular Imaging (2020) 54:207–223
https://doi.org/10.1007/s13139-020-00665-4

REVIEW

ISSN (print) 1869-3482
ISSN (online) 1869-3474

Brain Glymphatic/Lymphatic Imaging by MRI and PET

Dong Soo Lee[1,2] · Minseok Suh[1,2] · Azmal Sarker[2] · Yoori Choi[1,2]

Received: 2 June 2020 / Revised: 9 August 2020 / Accepted: 19 August 2020 / Published online: 27 August 2020

Abstract

Since glymphatic was proposed and meningeal lymphatic was discovered, MRI and even PET were introduced to investigate brain parenchymal interstitial fluid (ISF), cerebrospinal fluid (CSF), and lymphatic outflow in rodents and humans. Previous findings by ex vivo fluorescent microscopic, and in vivo two-photon imaging in rodents were reproduced using intrathecal contrast (gadobutrol and the similar)-enhanced MRI in rodents and further in humans. On dynamic MRI of meningeal lymphatics, in contrast to rodents, humans use mainly dorsal meningeal lymphatic pathways of ISF-CSF-lymphatic efflux. In mice, ISF-CSF exchange was examined thoroughly using an intra-cistern injection of fluorescent tracers during sleep, aging, and neurodegeneration yielding many details. CSF to lymphatic efflux is across arachnoid barrier cells over the dorsal dura in rodents and in humans. Meningeal lymphatic efflux to cervical lymph nodes and systemic circulation is also well-delineated especially in humans onintrathecal contrast MRI. Sleep- or anesthesia-related changes of glymphatic-lymphatic flow and the coupling of ISF-CSF-lymphatic drainage are major confounders ininterpreting brain glymphatic/lymphatic outflow in rodents. PET imaging in humans should be interpreted based on human anatomy and physiology, different in some aspects, using MRI recently. Based on the summary in this review, we propose non-invasive and longer-term intrathecal SPECT/PET or MRI studies to unravel the roles of brain glymphatic/lymphatic in diseases.

Keywords Interstitial fluid · Cerebrospinal fluid · Glymphatic · Meningeal lymphatic · Imaging.

Introduction

Brain glymphatic was proposed in 2012 by Iliff and colleagues to explain waste clearance from the brain parenchyma [1]. In 2015, Louveau and colleagues found the existence of meningeal lymphatics and suggested that meningeal lymphatic can clear wastes from the brain [2]. Afterward, there had been many efforts to link glymphatic clearance [3–12] and lymphatic drainage in small animals and humans [12–17]. Now, interstitial fluid (ISF) is drained to cerebrospinal fluid (CSF) [1, 3] (Fig. 1), and further drainage of CSF to meningeal lymphatics are well-established [12, 13, 22] (Fig. 2). CSF is considered to drain via dorsal lymphatic vessels; basal lymphatic vessels [2, 4, 12–14, 17, 25–27], along the nerve sheaths of olfactory and other cranial nerves [27–31]; and spinal meningeal lymphatics [28, 32–34] (Fig. 3). Deep cervical lymph nodes were shown to receive fluorescent dye-labeled macromolecules [1, 15, 30, 36], radioisotope-labeled proteins (albumin or amyloid) [37, 38], and gadolinium-labeled magnetic resonance imaging (MRI) contrast agents [25, 39, 40], most prominently from CSF when they were injected to subarachnoid spaces at cisterna magna in rodents or intrathecally between 4th and 5th lumbar spines in rodents and humans.

On radioisotope (RI) cisternography [41], intrathecal injection of In-111 diethylenetriamine pentaacetic acid (DTPA) (or Tc-99m DTPA) has long been used to visualize the gross circulation of CSF over the spinal cord to reach basal cistern, around the hemisphere, to Sylvian, and interhemispheric cisterns to be washed out to the systemic circulation (Fig. 4). Arachnoid villi were supposed to receive all the radiopharmaceuticals from the CSF space but now they are known to drain only a small fraction of the CSF. On MRI in humans [44] (Fig. 4c), CSF was found to flow in a complex way meaning that CSF is produced from choroid plexus of the ventricles and flow out to foramen of Monro, via the third ventricle through

✉ Dong Soo Lee
dsl@snu.ac.kr

[1] Department of Nuclear Medicine, Seoul National University College of Medicine, Seoul 03080, Republic of Korea

[2] Department of Molecular Medicine and Biopharmaceutical Sciences, Graduate School of Convergence Science and Technology, and College of Medicine or College of Pharmacy, Seoul National University, Seoul 03080, Republic of Korea

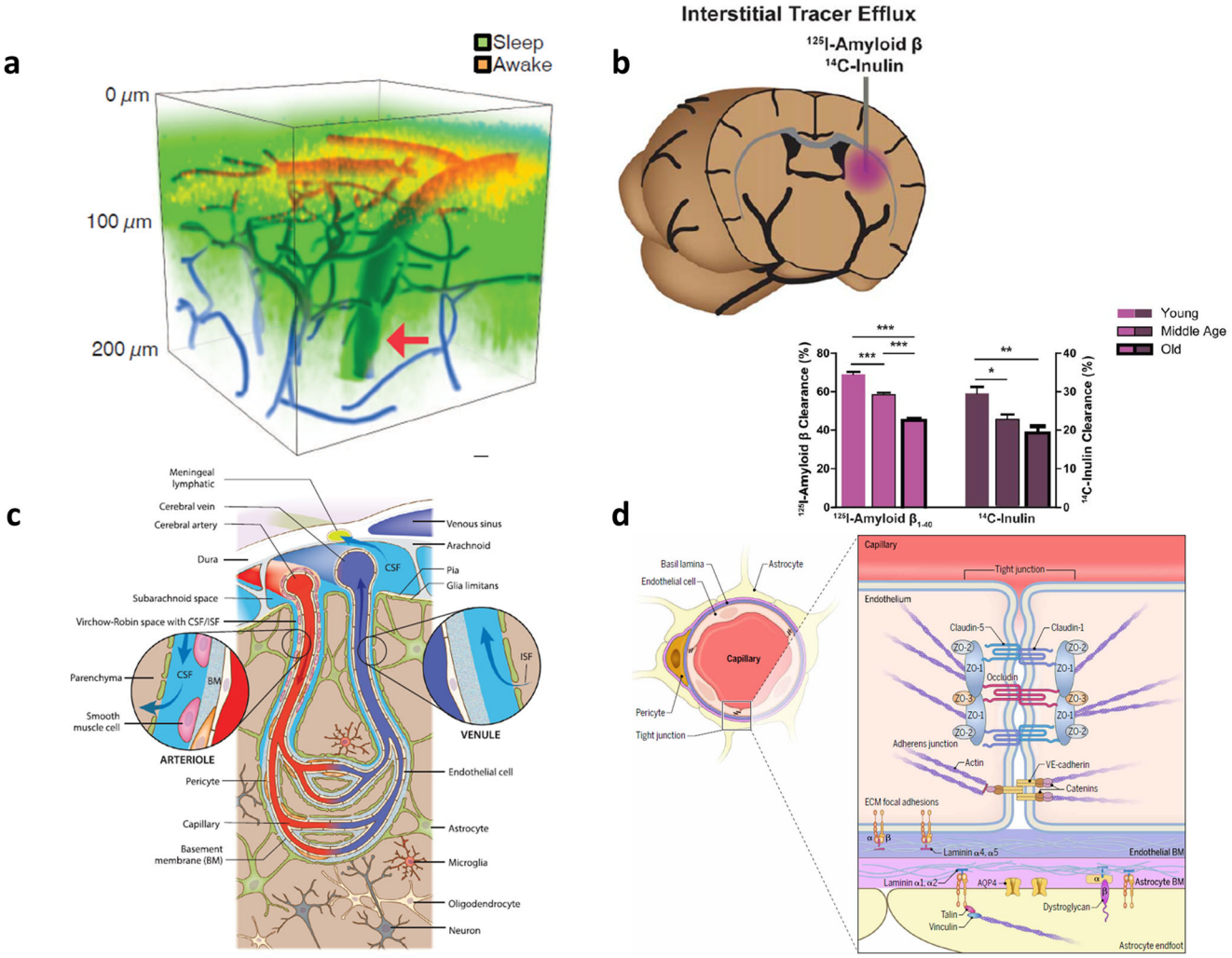

Fig. 1 Interstitial fluid (ISF)-cerebrospinal fluid (CSF) space connection. Glymphatic hypothesis and their experimental evidence in rodents. **a** Via cisterna magna cannula, during sleep at noon FITC-dextran (3 kDa, green), was given, and after being awakened 30 min later, Texas-red-dextran (red) was given. On in vivo two-photon microscopy, deeper/broader fluorescence during sleep and reduced fluorescence after being awakened were interpreted to represent the CSF influx of intra-cisternal administered small molecules. Reprinted with permission from Xie et al. [18]. **b** To ISF space of caudate nucleus via guide cannula, I-125 amyloid-beta and C-14 inulin were injected, and 60 min later, the radioactivity of the brain was measured to yield (100%-brain recovery) as percent clearance. ISF clearance decreased upon aging. Reprinted with permission from Kress et al. [19]. **c** ISF-CSF space is communicating through the basement membrane of the endfeet of astrocytes surrounding brain blood vessels through perivascular spaces (periarteriolar and perivenular spaces are well-documented and pericapillary space is supposed between basement membranes of astrocytic endfeet and vascular endothelial cells. Pericytes are located in this space. Reprinted with permission from Da Mesquita et al. [17]. **d** Schematic magnification of endothelial and astrocytic basement membranes. Reprinted with permission from Mastorakos and McGavern [20]. If periarteriolar and perivenular spaces filled with CSF are supposed to be connected with pericapillary spaces between basement membranes, the CSF network around parenchymal vessels was expressed as a circuit of paravascular spaces running CSF flow throughout brain parenchyma. Reprinted with permission from Coles et al. [21]

the aqueduct, to the fourth ventricle and via foramina of Luschka and foramen of Magendie to reach basal cistern. However, this flow was found to be to-and-fro especially in the aqueduct [46] (Fig. 4d). Vector imaging of proton MRI of the CSF fluid also showed that flow was accelerating/decelerating, changing directions, and was different between locations (ventricles and subarachnoid spaces) [45, 47] probably in order to make it easier to wash out the perivascular spaces of regional brain parenchyma.

It is found that in rats, the basal meningeal lymphatic vessels are different in the architectonics of lymphatic endothelial cells which differed in aging-related changes [27] (Fig. 3a). With this finding, Ahn and colleagues [27] speculated that this difference reflected the fact that the main route of CSF drainage was via basal lymphatics as well as along the olfactory nerves/cribriform plates [27, 48]. This was in accord with many of the previous studies which used fluorescent dye-labeled materials [12–14]. However, the most recent finding

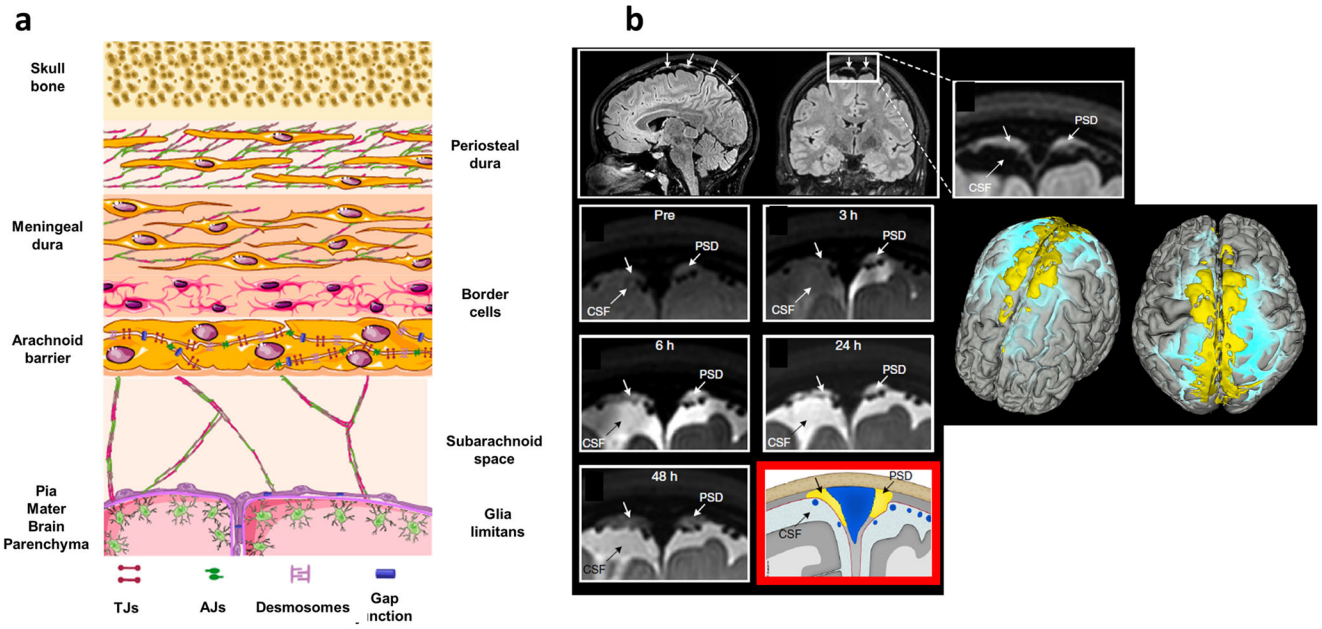

Fig. 2 CSF efflux to meningeal lymphatics. CSF and their solutes pass through arachnoid barrier cells to reach parasagittal dura. **a** On this schematic representation of meningeal layers, the arachnoid barrier layer is considered to be composed of cells of epithelial/mesothelial origin which have tight junctions. Reprinted with permission from Castro Dias et al. [23]. Tight junctions of arachnoid barrier cells have claudin-2 and aquaporin-1 (AQP1) like choroid plexus epithelial cells capable of passing water among various isoforms of claudins [8, 23]. **b** Forty-eight hours after gadobutrol (604 Da) injection, 3D T2-FlAIR MRI image reveals parasagittal dura (yellow) and CSF (light blue) on the segmented brain. Coronal serial T2-FLAIR images before and 3 to 48 h after intrathecal injection of gadobutrol show CSF tracer efflux to this parasagittal dura in humans. The blue triangle on the red box image represents superior parasagittal sinus. Reprinted with permission from Ringstad and Eide [24]

on MRI, which traced the whereabouts of intrathecally injected contrast agents, was against this speculation [24]. In humans, dorsal meningeal vessels seem to take a major role in clearing the wastes from ISF-CSF (Fig. 2b). Thus, differences among species should be considered when interpreting CSF-lymphatic drainage. In humans, internal carotid artery–derived pial arteries are not directly connected to meningeal arteries; instead, they supply substrates via blood-brain barrier to the brain parenchyma, and then, the excess, surplus, and metabolites are disposed from ISF space via glymphatic to CSF. Those solutes of CSF are cleared to meningeal lymphatics via the pathways described in detail above and below.

Contrast-enhanced MRI showed its capability to reveal the detailed CSF efflux after intrathecal injection, which mimicked the radionuclide cisternography (RI cisternography) in their findings [39, 40, 49–51]. Furthermore, it could be used to visualize the direction of CSF flow [44, 45, 47] (Fig. 4c), the direction of lymphatic flow compared with the venous flow [35], and even glymphatic flow along the glia limitans externa of the hemispheric pial surface [52]. In animals, MRI was also used to find the acute effect of anesthesia [53–56], sleep and wakefulness [46] (Fig. 3d), or even the drug treatment [57, 58]. A variety of manipulation influenced glymphatic flow, which was at first examined with fluorescent dye-labeled macromolecules [1, 3, 7, 15, 36] and then RI-labeled proteins on nuclear imaging/radioactivity counting [1] or contrast-enhanced MRI [24, 35, 39, 40, 49–60].

Here we explain the details of the current understanding of glymphatic and lymphatic imaging using MRI [24, 35, 39, 40, 49–60] and positron emission tomography (PET) [61, 62]. Relevant physiologic and pathologic status were also reviewed, which incurred the necessity to use MRI and PET in humans as well as in rodents. Among these statuses, sleep and dementia were the ones that were studied best in detail and current understanding was summarized. We also tried to unravel the possible theranostics implication of using MRI and PET to image glymphatic and lymphatic clearance in humans, as well as in small animal models.

Detailed Anatomy of Glymphatic Flow and Lymphatic Drainage

Fluorescent dye-labeled small- or intermediate-sized materials such as dextran could visualize perivascular spaces of brain parenchyma [1] (Fig. 1a). Periarteriolar space was well visualized by dual staining on fluorescent microscopy after intracisternal injection of small molecular dextran and systemic administration of fluorescent intravascular agents for counterstaining vascular lumen [1]. Interestingly, perivenular space showed asymmetric localization of venule within perivenular space, which was simply considered a tissue-fixation artifact during pre-processing for microscopy [21]. Expectedly, pericapillary space did not show up due to the

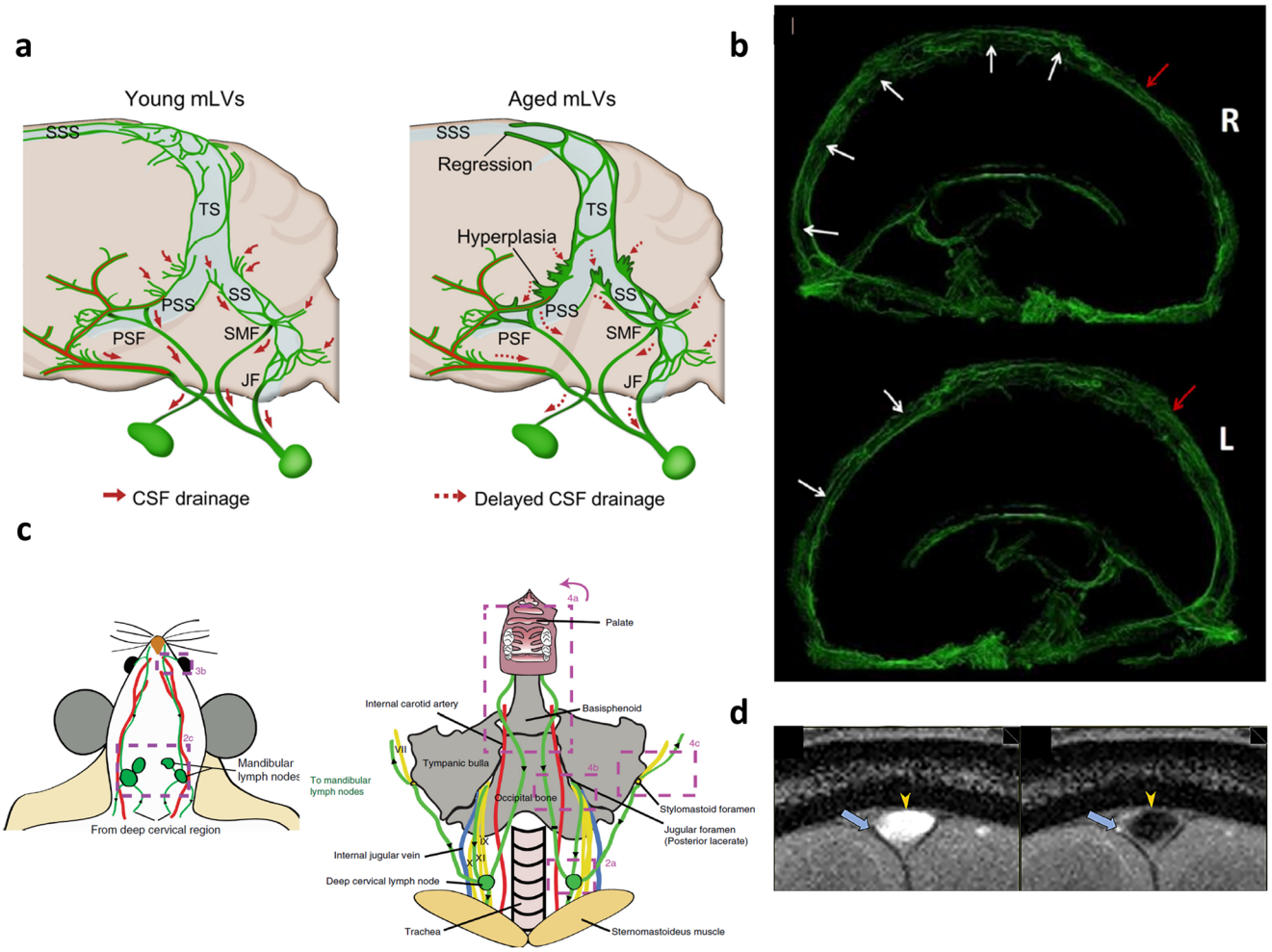

Fig. 3 The outflow of meningeal lymphatics in mice and humans. **a** In mice, on in vivo fluorescent microscopy and ex vivo histologic studies, zipper-like junctions in the young and button-like junctions are differentially found in dorsal (SSS: superior sagittal sinus, TS: transverse sinus) and in basal (SS: sigmoid sinus, PSS: petrosquamosal sinus), respectively. Aging resulted in hyperplasia, impaired valves, and disrupted junctions. PSF petrosquamous fissure, SMF stylomastoid foramen, JF jugular foramen. Reprinted with permission from Ahn et al. [27]. **b** After intrathecal injection of gadodiamide, at 15 h, putative meningeal lymphatic vessels were visualized on these 3D CUBE-T2-FLAIR MRI images. Unenhanced superior sagittal sinuses (white arrows) were surrounded by putative meningeal lymphatic vessels. Reprinted with permission from Zhou et al. [22]. **c** On stereomicroscope in Prox1-GFP mice after intraventricular injection of infrared pegylated dye (40 kDa), the outflow of CSF was found to reach mandibular (superficial cervical) and deep cervical lymph nodes within an hour. The flow was followed through lymphatic vessels and shown as arrowheads on this schematic drawing. Reprinted with permission from Ma et al. [30]. **d** On T2 FLAIR MRI, TOF angiography was done to reveal the direction of the flow, saturation band posterior to the image section showed bright signal in superior sagittal sinus due to influx of unsaturated venous blood from anterior to posterior direction (left image; yellow arrowhead). In reverse, the saturation band anterior to the image section showed an expected low signal but the white signal in meningeal lymphatic vessels (right image: blue arrow). Countercurrent lymphatic flow from posterior to anterior compared with the venous flow was concluded in humans. Reprinted with permission from Absinta et al. [35]

same reason and/or postmortem loss of fluid from much smaller pericapillary spaces (Fig. 1c). Instead, endothelial basement membrane and astrocytic end-feet basement membranes were separately identified (Fig. 1d). Thus, investigators could imagine that periarterial, pericapillary, and perivenular spaces were all interconnected and the name of paravascular space circuit was given to this network [1, 4, 12, 20, 21].

The glymphatic hypothesis was conceived based on these observations that paravascular or at least periarteriolar and perivenular spaces would be used as the clearing routes of ISF to the extra-brain spaces probably via meningeal lymphatics [16]. To be exact, the initial proposal of glymphatic was based on the then-popular concept that there are no lymphatics in the brain [1, 28, 29, 32, 33]. This ignorance about the existence of meningeal lymphatics resulted in using "CSF influx" after intrathecal tracer injection [1] (Fig. 1a). In fact, fluorescent tracers administered intra-cisternly showed influx into the paravascular spaces varyingly. And now, CSF influx is the other face of ISA efflux which just depends on where the tracer was given, ISF space of brain parenchyma or ventricular/subarachnoid CSF space. When anesthesia or sleep was induced in mice, intrathecally

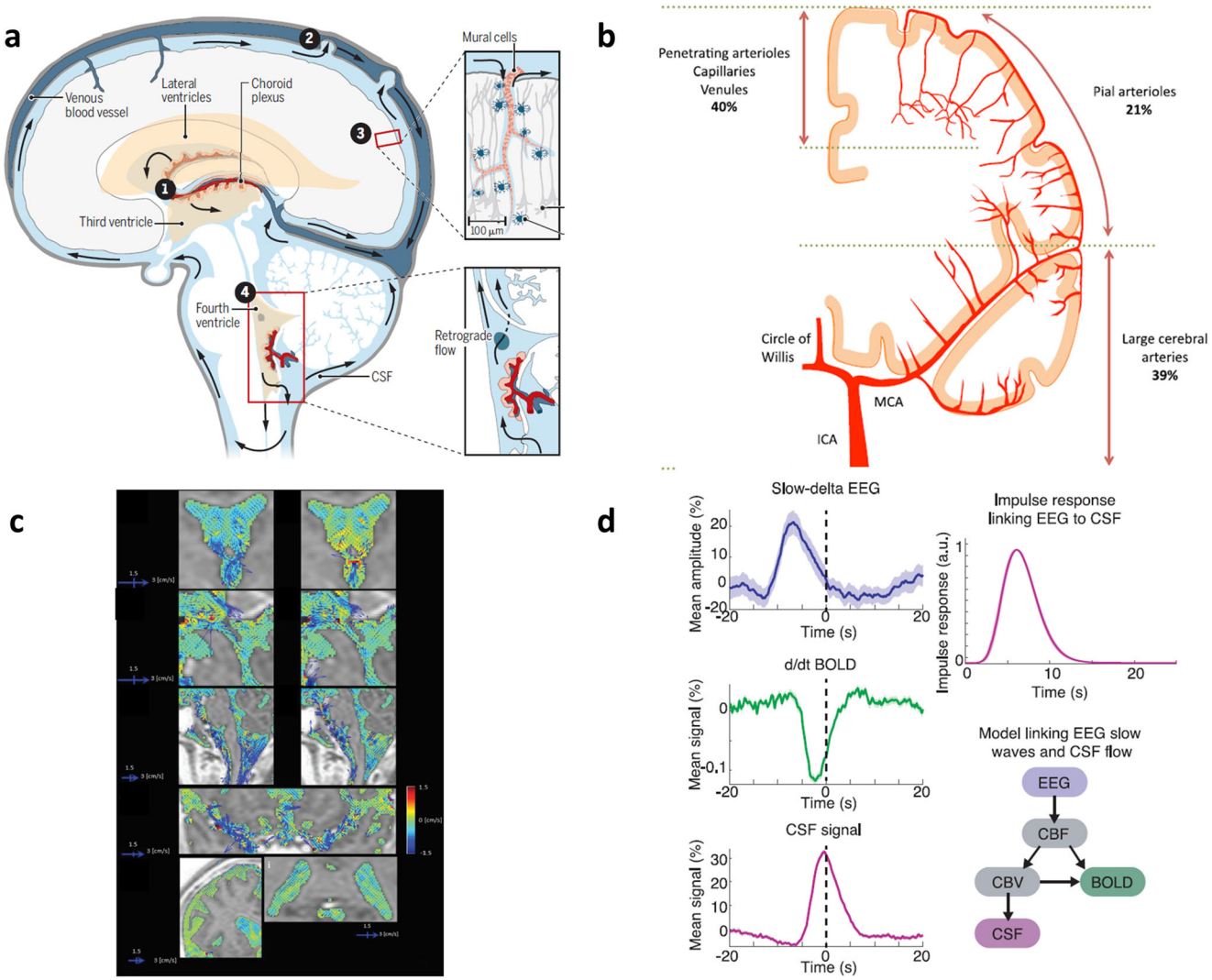

Fig. 4 CSF circulation in relation to parenchymal vessels. CSF was once considered to circulate but in fact, not. **a** Classic understanding of CSF flow produced from ventricles (lateral, third, and fourth), flowing out to cisterns and going down to the spinal canal and over the cord and returning to basal and inter- or over the hemispheric subarachnoid spaces to reach arachnoid villi to be absorbed. In this picture, the flow between the third and fourth ventricle is said to be found bidirectional. Aqueduct connecting third and fourth ventricles are open with this bidirectional flow. Reprinted with permission from Grubb and Lauritzen [42]. **b** Internal carotid artery supplies wider than anterior two-thirds of both cerebral hemispheres. Large or small, vessels outside of parenchyma are responsible for 60% of total resistance (39% + 21%) and penetrating arterioles and venules for the remaining 40%. Reprinted with permission from Iadecola [43]. **c** On 3D phase-contrast MRI images, CSF flow was found not to be circulatory, but complex, accelerating/decelerating, unstable, and augmented in the center of the cranial cavity of subarachnoid space, and third/fourth ventricles [44, 45]. Reprinted with permission from Matsumae et al. [44]. **d** On simultaneous measurements of EEG, BOLD on fMRI, and CSF flow dynamics imaging, during NREM sleep, slow delta wave (increased amplitude) preceded BOLD changes (decreased signal) which also preceded CSF flow oscillatory changes. NREM sleep with its impact upon hemodynamic status results macroscopic oscillations in fourth ventricle CSF. Reprinted with permission from Fultz et al. [46]

administered fluorescent tracers were found more widely in extent and deeply into the cortex than in awake state [1]. Intraparenchymal tracer was speculated to be cleared to the sinus veins in the dura, after passing through the ISF space to carry out the waste solutes therein via perivenular space to subarachnoid spaces. Two ideas, (1) fresh CSF arriving at the periarteriolar space pass through the parenchyma via perivenular space to subarachnoid spaces and (2) ISF-CSF exchange is the key process of solute clearance from brain parenchyma, were based on the assumption that arterial pulsation-driven convective flow is the driving force of this CSF-ISF-CSF washout [1, 3, 7, 9]. Several groups refuted this hypothesis saying that ISF does not need unidirectional convection flow to carry and clear waste solutes by providing simulation/observation results of their own [5, 10, 11, 63–65].

The seminal discovery of meningeal lymphatics enlightened investigators of this field recently [2]. It cleared concern which had bothered investigators for almost a hundred years because of the incorrect notion of an absence of meningeal lymphatics [8]. There is no more need to find the exit routes

falsely in charge of the efflux of CSF such as arterial sheath [33] similar to olfactory [27, 29, 30] or optic nerve sheath [28, 30, 31]. It is now known that these microstructures of cranial nerves also drain glymphatic in their capable amount, but the majority of ISF-CSF and brain parenchymal waste solutes are cleared via meningeal lymphatics [12, 13, 16, 17, 25]. "ISF efflux" could replace "CSF influx" in expressing the fluid (and the solutes/metabolites therein) turnover (Fig. 1a, b). If expressed sequentially, fluid/waste flux moves from brain parenchyma, ISF space, paravascular space, CSF space, dural peri-sinus space (Fig. 2b), and to meningeal lymphatics [66]. ISF efflux was found to be the largest during non-rapid eye movement (NREM) sleep with higher slow (delta) wave during sleep or anesthesia [66, 67] which later came to be believed to take the role of disposing such metabolites/solutes from the brain as adenosine, norepinephrine, other neurotransmitters/gliotransmitters, amyloid oligomers, and extracellular tau, either bare or within extracellular vesicles. And thus, on dynamic MRI, tracers administered intra-cisterna magna could not easily redistribute to the paravascular spaces of the cortex represented traditionally as CSF influx. This less redistribution or less CSF influx was interpreted to be due to the increased ISF efflux in the day, light phase during sleep of the rats [66]. This redistribution was interestingly varied from region to region, that is to say, dorsal cortex showed the similar redistribution of tracers between light and dark phases (sleep and wake phases) while midbrain/pons and ventral cortex showed decreased redistribution during sleep than in awake state in rats [66]. This was contradicting the initial report that the CSF influx was wider and deeper during sleep or anesthesia than the awake state on two-photon imaging [18] (Fig. 1a). Initially, the CSF influx was more during sleep [18] on skull-window in vivo fluorescent microscopy study after cisterna magna infusion, but CSF influx was less during sleep on intraventricular contrast-enhanced MRI [66]. Beside many confounding factors such as head position, anesthesia, sleep, circadian phase, and others, short-term observation and time differences might be considered for understanding the subtle changes of glymphatic flow. Of course, the complexity of CSF flow should be considered in that CSF flow is not circulatory but bidirectional, accelerating and/or decelerating [66] (Fig. 4c).

Sleep-Related Physiologic Fluctuation of Glymphatic and CSF Flow (Fig. 5)

Sleep consist of NREM and rapid eye movement (REM) sleep [72], and this classification was meaningfully physiological for brain waste disposal with the NREM- and REM-specific characteristic electroencephalographic waves [18, 67]. Slow delta waves are associated with glymphatic flow [18, 54, 67, 69, 73]. Amplitudes of slow delta waves during NREM sleep were repeatedly found to be related with the effective waste disposal in rats [18, 67, 69, 73]. Sleep deprivation resulted in the stalled glymphatic flow and the accumulation of waste solutes including beta-amyloid solutes in the brain as well as adenosine and others [68, 73–76]. Sleep deprivation could kill the animal if prolonged, and investigators assumed that toxic amyloid oligomers and extracellular pathologic tau were to be cumulated [73, 77, 78], due to sleep deprivation-related glymphatic dysfunction, to evoke the neuroglial dysfunction in Alzheimer's disease (AD) model animals [77, 78] and also in humans [74, 75] (Fig. 6).

During sleep, glymphatic flow is increased by the action of astrocytes using aquoporin4 [5, 7, 8, 80]. Astrocytes are unique in their cytoarchitectonics making a functional syncytium-like reticular network that conveys lactates produced during wakefulness (during dark night in rodents) [57, 70, 71, 81] (Fig. 5c) and making barrier using their end-feet against vascular channels (glia limitans) and pial surfaces of cortices (glia limitans externa) [8, 43, 71] (Fig. 2a). The functional syncytium feature enabled by the connexin junction between neighboring processes of astrocytes is the platform of the concentration-dependent diffusion-based stationary phase of the astrocyte reticular network [57, 70, 81, 82] (Fig. 5c). Lactates are excreted easily to paravascular spaces during sleep using this syncytium-like structure and astrocytes are considered to be responsible for the modulation of phases between sleep and awake states [81]. End-feet aquaporin4 (AQP4), proposed for their essential contribution to glymphatic transport [7], plays an essential role as these move water between intracellular space and interstitial space [80]. Using membrane channel protein AQP4 and water flux through AQP4 [80], astrocytes can shrink the cell volume of brain parenchyma to increase ISF space from 14% during wakefulness to 23% during sleep [18]. This widened ISF space suit better so the water and solutes therein could diffuse to adjacent paravascular space. According to the recent measurement of the number of glial cells and neurons in the cortex (i.e., cerebrum and cerebellum) [83], the ratio of glial cells to neurons was 4:1 in the cerebrum and 1:4 in the cerebellum. Thus, the global ratio of astrocytes to neurons was 1:1 [84]. The gap junction between astrocytes wrapping the brain vessels (mainly capillaries) is now ready to pass the ISF contents of water and solutes to paravascular space [8]. Once in the paravascular space, ISF containing solutes are ready to be delivered to subarachnoid space by efflux of paravascular CSF compensating CSF influx which is used to be observed in intra-cistern/intraventricular fluorescent microscopy [18] or MRI [54].

During NREM sleep, ISF and its contents are cleared to CSF in paravascular and subarachnoid spaces, and this CSF is believed to cross arachnoid barrier cells to reach dural ISF space to arrive at the lymphatics (Fig. 2b). These arachnoid barrier cells are also equipped with claudin-2 for their tight junction and AQP1 [8, 23], as claudin-2 is capable to pass water

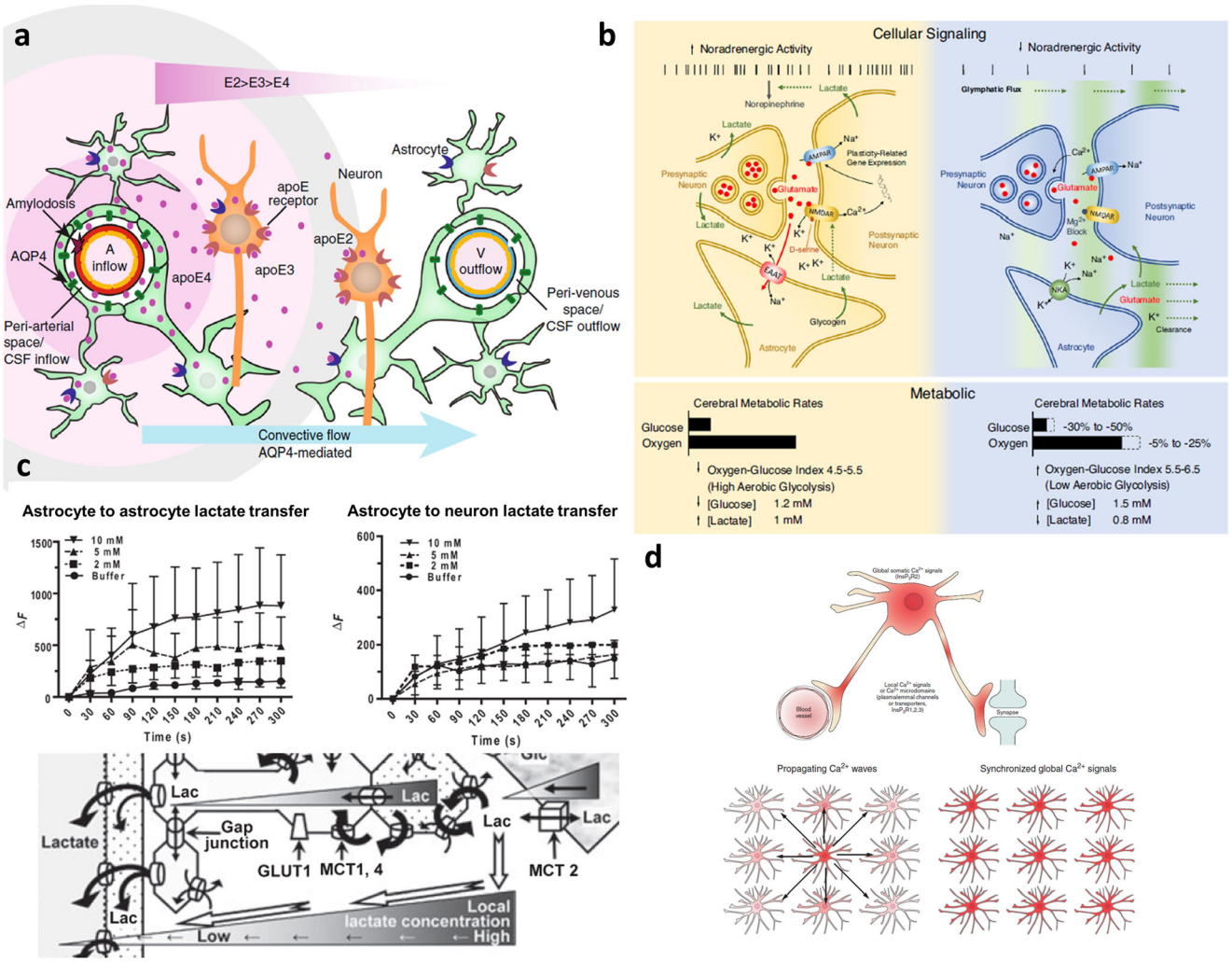

Fig. 5 Coupled ISF-CSF-lymphatic efflux and the objectives of this efflux. **a** Mice in which lenti-ApoE was delivered to their choroid plexus released ApoE to the CSF and ApoE contained in CSF was delivered to the periarteriolar space. ApoE in CSF convective flow revealed that the extent of convective/bulk flow into the ISF around the arterioles was isoform-dependent. ApoE2 diffused farther than ApoE3 which is also farther than ApoE4. This is evidence of the ISF influx from CSF. Reprinted with permission from Achariyar et al. [68]. **b** Wake-sleep cycle dictates cell signaling between neuron-neuron-astrocyte couples. While awake, extracellular K^+ is increased under norepinephrine effect, and lactate is produced more and released with preferred aerobic glycolysis. During sleep, lactate, K^+ as well as glutamate are cleared with glymphatic/lymphatic drainage while glucose consumption decreases more than oxygen consumption (less aerobic glycolysis). Reprinted with permission from DiNuzzo and Nedergaard [69]. **c** Astrocytes are coupled with astrocytes to make a reticular system. One of the impacts of this reticular system is that lactate transfer from astrocyte to astrocyte is greater and faster and that from astrocyte to the neuron is smaller. A larger volume of dilution and concentration gradient enables intracellular lactate to diffuse to paravascular fluid space. Extracellular lactate is also cleared to paravascular spaces due to the concentration gradient. Reprinted with permission from Gandhi et al. [70]. **d** Syncytium-forming astrocytes show propagating Ca^{+2} waves which are fast enough to explain long-range information transfer and even to make global synchronized global Ca^{+2} signals. Reprinted with permission from Verkhratsky and Nedergaard [71]

molecules by the support of AQP1 unlike the other claudins [23] (Fig. 2a), implying that they are also able to control the water passage from subarachnoid space to the space of dura harboring sinus veins and meningeal lymphatics vessels. As lymphatic endothelium is easy for the water-carrying solutes/metabolites to pass [85], ISF-CSF contents reach the lumen of meningeal lymphatic vessels and are slowly drained via the deep lymphatic vascular networks of the neck. Thus, during sleep especially the NREM phase [86–88], under the delta wave association [46, 67] (Fig. 6b), increased ISF space [18], and opened gap junction of astrocyte end-feet network [81], ISF and CSF are likely to be mixed, as if without barrier at that moment [4, 6, 8] and according to the concentration gradients of the contents amenable to be cleared. CSF and lymphatics are believed to behave in the same way during sleep. Only one reserve is that sleep takes time, and thus, acute effect and prolonged effect of sleep should be cautiously interpreted. Fluorescent tracer [1, 3, 7, 12–15, 36] or contrast-enhanced MRI studies [25, 39, 40, 46, 53–58] mostly looked for the acute effect ranging from 30 min to hours.

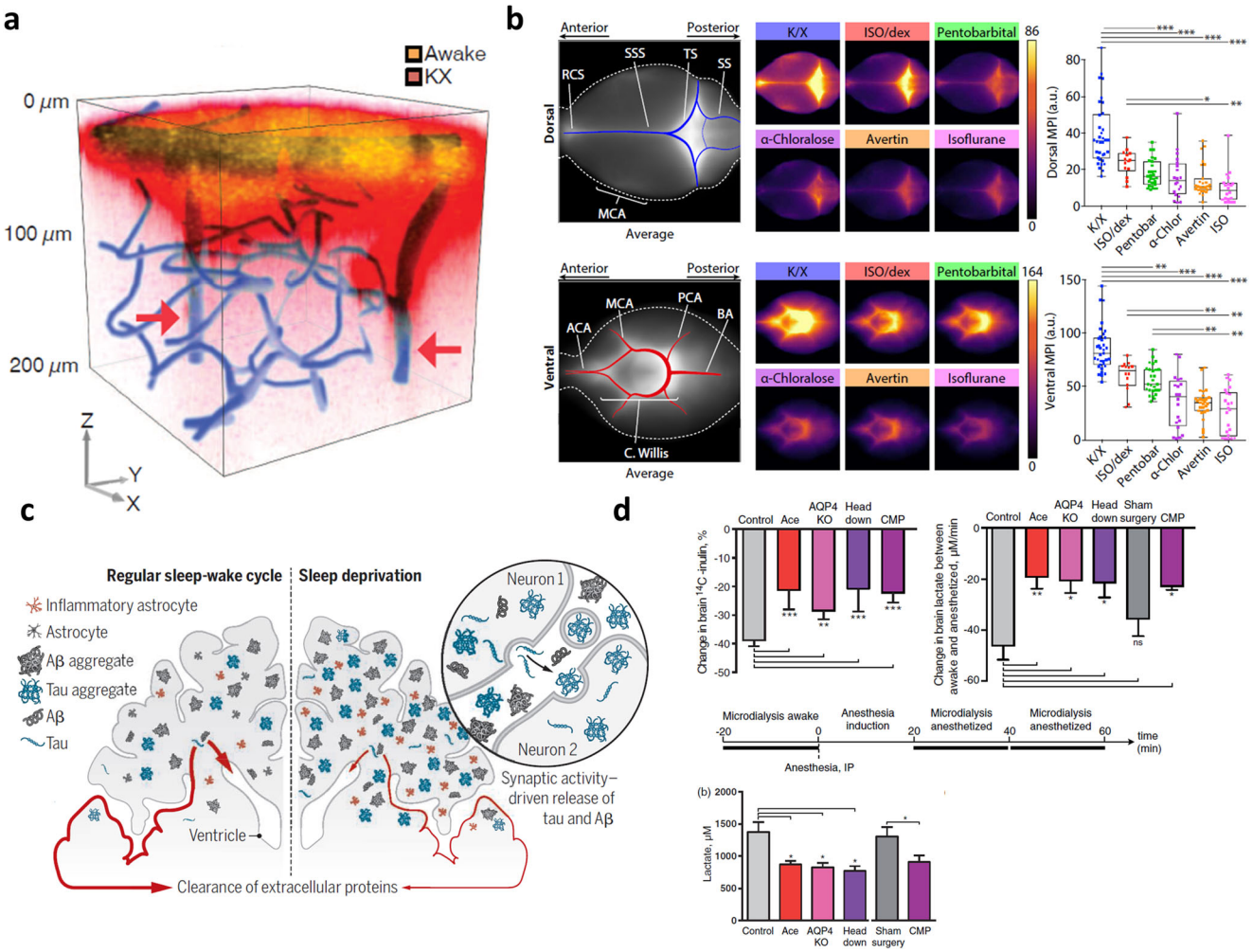

Fig. 6 Effect of sleep or anesthesia on ISF-CSF-lymphatic efflux. **a** Via cisterna magna cannula, during awake in the night, fluorescent dye was given, and after ketamine/xylazine anesthesia, another fluorescent dye was given. On in vivo two-photon microscopy, deeper/broader fluorescence during ketamine/xylazine anesthesia mimicked sleep to represent CSF influx. Reprinted with permission from Xie et al. [18]. **b** However, when individual anesthetic drugs were compared regarding their effect on glymphatic (CSF influx), 30 min after intra-cisternal injection of fluorescent albumin (66 kDa), the brain was removed for ex vivo fluorescence microscopy to yield a variety of responses to the glymphatic flow. GABAa and receptor modulators, i.e., isoflurane (ISO), alpha-chloralose (alpha-Chlor), and others showed a decrease in albumin distribution in ventral/dorsal CSF spaces. Alpha-2-adrenergic agonists (alpha-Chlor), dexmedetomidine (dex), and xylazine (with NMDA receptor antagonist ketamine: K/X) showed less but also decrease. Their decrease in CSF albumin distribution was related to slow-wave delta power under anesthesia meaning that higher delta power under anesthesia indicated greater distribution of intra-cisternal albumin. MCA middle cerebral artery, ACA anterior cerebral artery, PCA posterior cerebral artery, BA basilar artery, RCS rostral confluence of sinuses, SSS superior sagittal sinus, TS transverse sinus, SS sigmoid sinus. Reprinted with permission from Hablitz et al. [67]. **c** Sleep deprivation was proposed to promote Alzheimer's pathology by impairing waste disposal from brain parenchyma via the ISF-CSF-lymphatic efflux system. Abeta oligomers and extracellular pathologic tau (free or within exosomes) should have drained from the ISF of the brain. Reprinted with permission from Noble and Spires-Jones [79]. **d** Using microdialysis in mice, ISF lactate amount was measured during awake and anesthesia and the difference of lactate between two states were considered to represent the effect of influencers such as acetazolamide infusion (Ace), aquaporin 4 knock-out (AQP4 KO), head down and cisterna magna puncture (CMP). The severe effect was observed on the decrease by ACE/CMP meaning less decrease of drainage during anesthesia. This decrease in anesthesia-induced decline was suggested to be due to impaired glymphatic function. This was corroborated by the decreased lactate amount in the deep cervical lymph nodes. Reprinted with permission from Lundgaard et al. [57]

During sleep, CSF was found to oscillate in their direction of the flow in the fourth ventricle on a recent ingenuous MRI study [46] (Fig. 4d). Simultaneously measured cerebral blood flow (CBF) disclosed the decrease of CBF around 10% during sleep compared with CBF during wakefulness [42, 46] (Fig. 4a). That decrease in CBF was associated with reduced cerebral blood volume and increased backflow through the aqueduct from the fourth ventricle to the third ventricle which made the to-and-fro flow called oscillation. Like these ventricles, all the other CSF flows should not be considered to be one-way; instead, there might be a global flow and the variety of local flows taking care of the regional needs and outlets

[44–47] (Fig. 4c). CSF surrounding spinal cords especially lower, i.e., lumbar or thoracic ones, would not have reason to flow over the hemisphere to reach arachnoid granulation within the superior sagittal sinus. They have their own meningeal lymphatics to clear the local waste products via spinal meningeal lymphatics [34, 36, 37].

Aging- and/or Neurodegeneration-Related Variances of Lymphatic Flow

When the scientific community had not recognized the presence and role of meningeal lymphatics for brain waste clearance, limited sources like ApoE, clusterin (ApoJ) [89–92], or other neuronal or cellular and molecular predisposition to age-related changes and neurodegeneration were brought to explain individual differences for brain aging and disease [90, 93–95]. Once, meningeal lymphatics came to be known, lymphatics' possible varied regression upon aging came to be another major source of differences between individuals. In animals, this was clearly reported as the dorsal meningeal lymphatic vessels regressed at the anterior part of the head [27] (Fig. 3a). This indicates that the regressed part of lymphatics at the anterior is the distal side. This assumption might be correct until MRI discloses the direction and age-related changes of lymphatic flow in rodents. In humans, direction and the importance of parasagittal dura space were discovered and found to be different from mice [24, 35] (Fig. 3b, d).

Aging-related regression in meningeal lymphatics, if any, would be the predisposing factor for the accumulation of toxic solutes of beta-amyloid and extracellular tau. Amyloid is a well-known extracellular solute that causes dysfunction and damage to the neurons when administered as synthetic or purified forms to the brain [96, 97]. And extracellular tau, either truncated, mutant, or phosphorylated forms within extracellular vesicles or in bare forms, is known to cause dysfunction of the neurons [93, 94, 97–101] or sequential recruitment of glial cells to cause further damage to the neurons [102, 103]. Interesting was the cumulated fact that amyloid plaques or neurofibrillary tangles might be innocuous per se and rather the toxic amyloid solutes and pathologic extracellular tau are the real culprit to inflict cascade damages to the neurons [99, 104–106]. According to the contributing roles of toxic amyloid solutes and pathologic extracellular tau, there were two hypotheses, amyloid cascade hypothesis and dual cascade hypothesis, which are not exclusive but different [107]. Obviously, the dual cascade hypothesis is the newer one receiving interests from investigators after the failure reports of almost all the clinical trials using anti-amyloid monoclonal antibodies for passive immunization [108–110].

The clearance of toxic amyloid solutes and pathologic extracellular tau is supposed to take place by four different plausible mechanisms [89, 90], which are (1) protease and enzymatic activity in situ within or outside of the neurons, (2) by the support of the other neurons or more likely the damage-associated microglia also in situ, (3) clearing especially amyloid combined with lipidated ApoE via low-density lipoprotein receptor-related protein 1 (LRP-1) expressing astrocytes/vascular endothelial cells [91, 102, 111], or (4) ISF-CSF-lymphatic clearance [1–8, 12–17, 22, 25–27, 112]. Each mechanism is now individually well-established and their unique contribution had been emphasized by each scientific community at various periods recently. However, their partial contribution and fraction of the roles in clearing the toxic protein solutes are not clarified yet. We can comment on the recent reports by stressing that the ISF-CSF-lymphatic clearance has a definitive anatomical foothold. The partial contribution of the ISF-CSF-lymphatic channel to the clearance of pathologic proteins and other metabolites is of great interest as it can contribute to the mitigation of the progress of AD if the methods of good choice are available to influence the efficiency of this pathway. Preservation of slow-wave NREM sleep [73, 79] is one example of preventive therapy against AD development with aging (Fig. 6c).

Aging-related paravascular clearance was reported before the discovery of meningeal lymphatics [19] (Fig. 1b and Fig. 7a), and aging-related impairment of CSF-lymphatic flow was documented in mice recently [30] (Fig. 3c). However, neurodegeneration-related impairment of CSF-lymphatic flow was not yet reported in AD mouse models. CSF-lymphatic drainage was definitely decreased in aged mice; however, this might be caused by the decreased CSF production due to choroid plexus dysfunction or larger space/volume of ISF in aged mice. A definite answer is warranted [30].

Abeta and tau should be cleared like other metabolites such as adenosine and norepinephrine [18, 46] from ISF via CSF through meningeal lymphatics to the systemic circulation [73, 78, 113] (Fig. 7b). This pathway of clearance has recently been established in its anatomical detail [2, 27] and physiologic fluctuation [42, 46]. Along with the exponential advance of discovery and interpretations about the clearance pathways of the last 5 years, the difference between humans and mice was disclosed [25, 27, 35], and the speculations showed up regarding the importance of the contribution of these pathways to the pathogenesis of AD [15, 113–116] (Fig. 8d). AD had been associated with sleep problems, and sleep disorder-related clearance dysfunction was revealed, and the possibility of prevention of AD by controlling sleep pattern was raised [46, 66, 74, 79, 118] (Fig. 6c). Furthermore, modulation of clearance of toxic solutes in the ISF was tried using focused ultrasound (FUS) [119–125] or continuous theta-burst stimulation (cTBS, a form of repetitive transcranial magnetic stimulation (rTMS)) [126]. Again, aging-related changes of these pathways were proposed to explain the variance of the susceptibility or disease courses of mild cognitive impairment converting to AD [22, 127]. The encounter of the waste

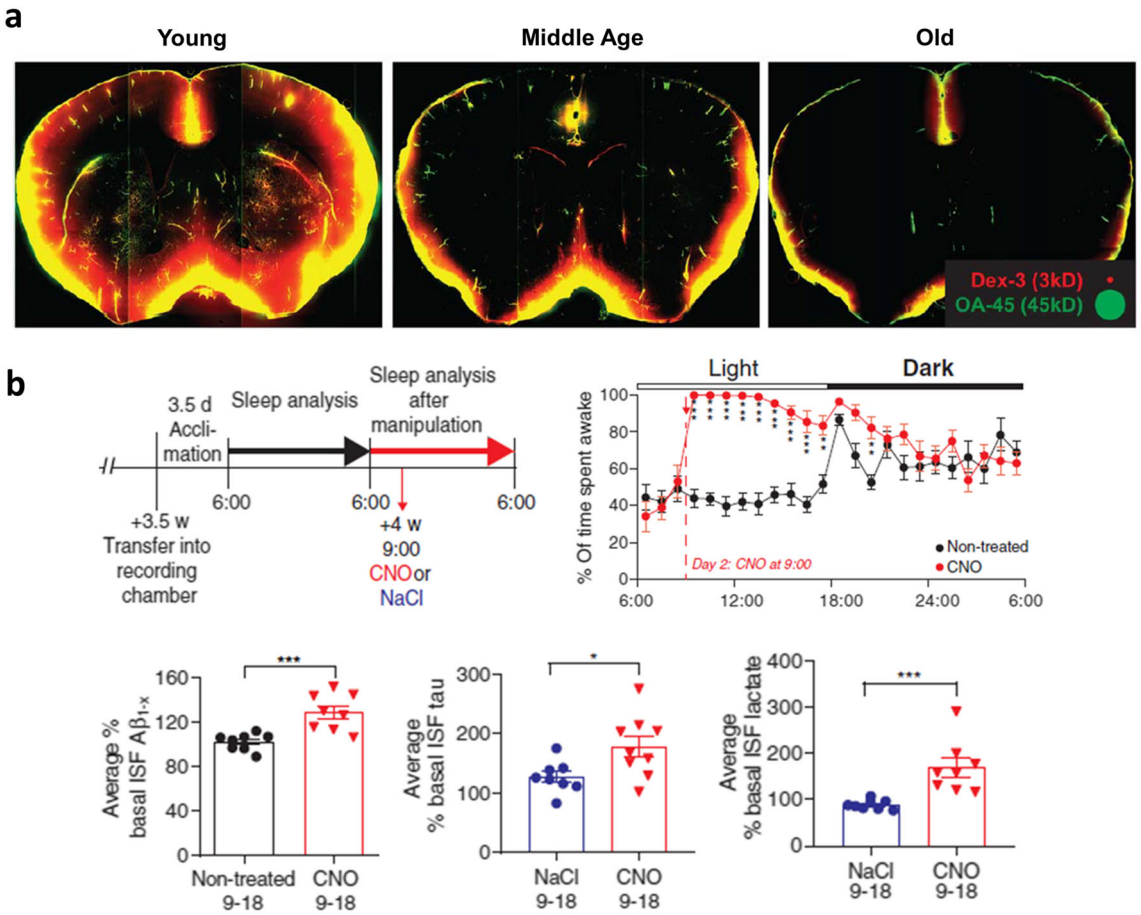

Fig. 7 Effect of aging and/or neurodegeneration on ISF-CSF-lymphatic efflux. **a** To cisterna magna, fluorescent ovalbumin was injected, and 30 min later, the brain was removed to evaluate whole slice fluorescence. CSF influx was decreased with aging. Reprinted with permission from Kress et al. [19]. **b** In a transgenic mouse having DREADD (designer receptors exclusively activated by designer drugs) hM3Dq, clozapine-N-oxide (CNO) was administered to let the mouse awake, and microdialysis revealed the increase in Abeta, extracellular tau, and lactate amount after CNO treatment. Associated with the findings that in humans, CSF tau increase 50% during sleep deprivation, sleep-wake cycle was suggested to regulate ISF abnormal proteins (Abeta and extracellular tau) and metabolites (lactate). Reprinted with permission from Holth et al. [78]

disposal with systemic innate and/or adaptive immunity is another recent add-up [128].

Similarity and Discrepancy of Glymphatic and Lymphatic Flow in Rodents and Humans

Studies in rats and mice and consequently in humans unraveled the anatomy and physiology of glymphatic and lymphatic flow [2]. In both species similarly to each other, lymphatics existed in the meninges (dura) and the cranial meningeal lymphatics are drained to the deep cervical lymph nodes [4, 12, 15, 16, 27, 33, 36, 57] (Fig. 8). CSF and dural meningeal lymphatics are bounded by arachnoid barrier cells and believed to allow the water and solutes from CSF to parasinus dural lymphatics [23] (Fig. 2b). Spinal dural lymphatic vessels are also believed to drain peri-spinal cord CSF [26, 32, 34] (Fig. 8b).

In mice, lymphatic vessels were found to have different shapes of endothelial architecture between basal and dorsal meningeal lymphatics, implying that the basal lymphatic endothelial cells have the structure for the water and solutes to pass more easily through the endothelium [27] (Fig. 3a). This finding easily resulted in the speculation that this is the anatomical background that the mice (and the rodents) are using the basal dural lymphatics to drain CSF as a stopover. The superficial layer of the head is drained to superficial lymph nodes such as mandibular or parotid lymph nodes [129], and these nodes again are drained to deep cervical lymph nodes [117, 130, 131] (Fig. 8c). After the administration of tracers to cisterna magna, the measured amount of tracers in the deep cervical lymph nodes represents the sum of drainage via meningeal lymphatics and via cranial nerves' sheaths (most well-known are the drainage along the olfactory nerves through cribriform plates [4, 12, 15, 16, 27, 33, 36].

In humans, lymphatic vessels were supposed at first to function similarly to rats and mice when the data were not

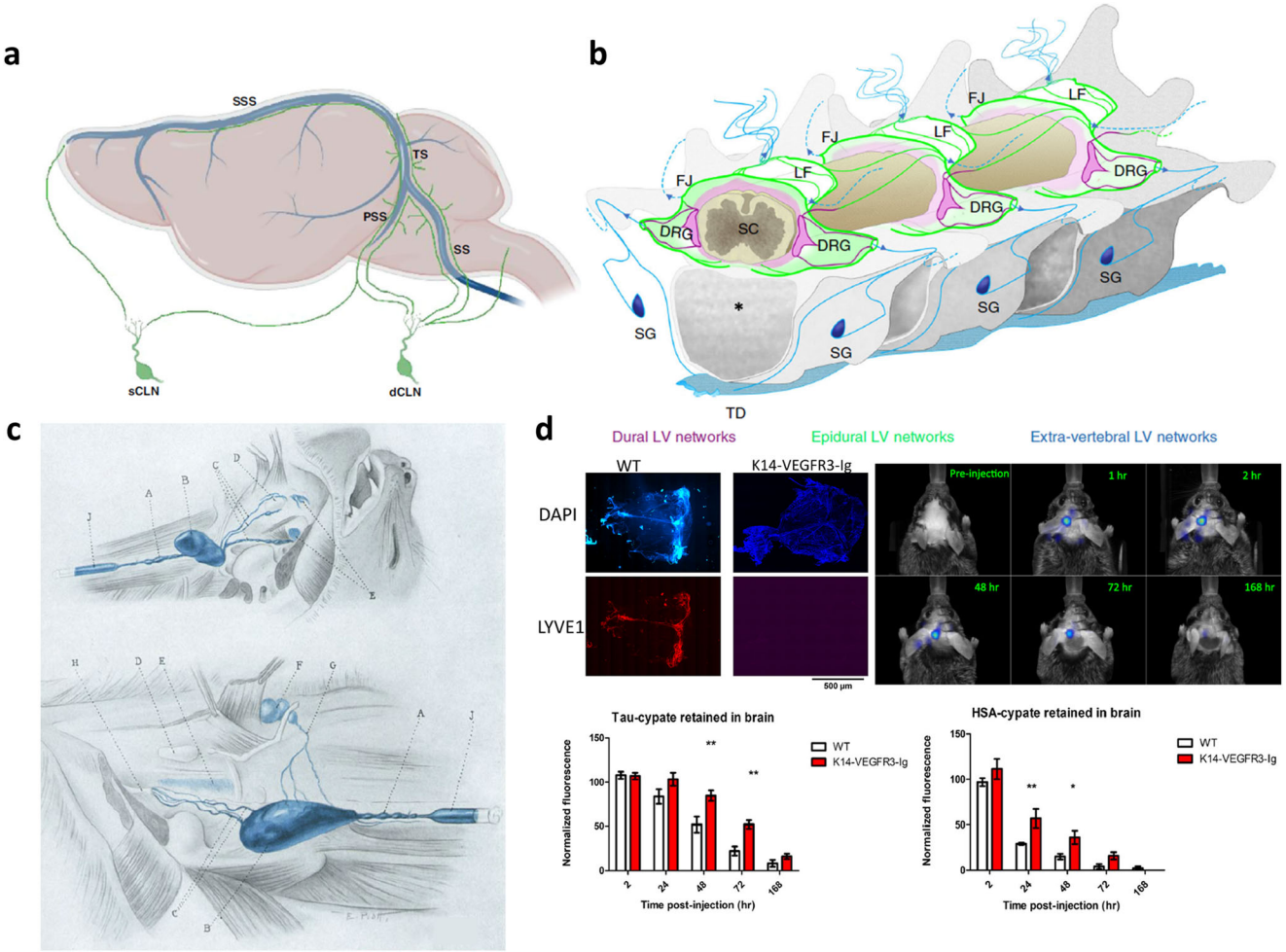

Fig. 8 Extracranial lymphatic drainage in mice. **a** Lymphatic vessels along petrosquamosal sinus (PSS) and sigmoid sinus (SS) exit skull via petrosquamosal fissure, stylomastoid foramen (with facial nerve), or jugular foramen (with cranial nerves IX, X, XI) to reach superficial cervical lymph nodes (mostly mandibular lymph nodes) or deep cervical lymph nodes. Upper cervical spinal lymphatics exit vertebra with dorsal nerve roots to reach deep cervical lymph nodes. How much of the CSF is drained to these two kinds of cervical lymph nodes is not known. Reprinted with permission from Frederick and Louveau [16]. **b** Spinal meningeal lymphatics were visualized using iDISCO+-clarified spine segments of lymphatic reporter mice. Dural lymphatic vessel (LV) networks (purple) and epidural LV networks (green) exit vertebral space to become extravertebral LV networks (blue) [34]. **c** Lymphatic pathway from meningeal lymphatics as well as from the nose and pharynx. A Cervical lymphatic duct. B Deep cervical lymph nodes. F Superficial cervical lymph nodes. G Lymphatic vessels connecting superficial and deep cervical lymph nodes. J Cannula in cervical lymph duct. Reprinted with permission from Yoffey and Drinker [117]. **d** In the K14-VEGFR3-Ig mouse model lacking superior sagittal and transverse sinuses (no structures in LYVE1 image), fluorescent tau and human serum albumin (HSA) cleared slowly after intrahippocampal injection. The kinetic difference shows the contribution of meningeal lymphatics and the contribution of other pathways such as along neural sheaths of olfactory, optic, trigeminal, IX, X, XI, etc. Reprinted with permission from Patel et al. [113]

available. However, recent investigations using MRI raised doubts against this assumption. Two findings in humans were definitely different from those in rats and mice: (1) dorsal lymphatic meningeal vessels drain most of the CSF and solutes therein in humans [24, 39] and there is yet to be found any evidence of CSF-lymphatic drainage through cribriform plates, if any, on MRI, (2) lymphatic flow was countercurrent to the superior sagittal sinus flow meaning that as sinus venous flow is anterior to posterior, posterior to anterior dorsal meningeal lymphatic flow is countercurrent to venous flow [35] (Fig. 3d). The latter fact is against the hypothesis that aging-related possible regression of the anterior part of dorsal lymphatics in humans, which was reported in a recent animal study [27]. In humans, the role of dorsal dural meningeal lymphatics is a point of extreme interest. CSF in the subarachnoid space, once having crossed lining of arachnoid barrier cells, would be mixed with peri-lymphatic vessels, and simultaneously peri-venous sinuses, and then drained to the meningeal lymphatic vessels of the cranium. These meningeal lymphatic vessels are to be drained via foramens and fissures of the skull and then via superficial cervical lymph node (mandibular lymph nodes) to deep cervical lymph nodes of the

neck. CSF contents are to encounter myeloid/immune cells, as a recent report told the plausibility that if CSF-contained solutes are drained to superior sagittal sinus, they might further be drained to the bone marrow sinuses of the dorsal skull [132]. In mice using in vivo cell labeling and ex vivo confocal microscopy, the vessels connecting the superior sagittal sinus embedded in the dura with the bone marrow of the skull were recently discovered.

MRI Studies to Reveal the Characteristics of Glymphatic and Lymphatic Flow

CSF-lymphatic drainage is now a well-established fact in rodents and in humans. Detailed anatomical understanding of meningeal lymphatics has led to the possibility of in vivo imaging and thus the repeated observation in vivo. For in vivo imaging, the methods should be non-invasive and are easy to repeat without perturbing the stationary state of the subjects, either rodents or humans [60]. Chronologically speaking, intraventricular contrast dynamic CT [48], gadobutrol/gadofosveset-enhanced T2-FLAIR/T1 MRI [50], 7-T FLAIR MRI [52], intrathecal gadobutrol MRI [39], dynamic contrast-enhanced (DCE) MRI using gadodiamide [59], quantitative DCE MRI [51], SPACE FLAIR/T2/TOF MRI of the superior sagittal sinus [35] (Fig. 3d), contrast FLAIR MRI for glymphatic visualization [125], and gadodiamide T1/T2 FLAIR MRI [22] (Fig. 3b) even for the simultaneous glymphatic and lymphatic vessels. CSF fluid efflux to parasagittal dura was unraveled with T1 black-blood and intrathecal DCE T1 MRI with intrathecal gadobutrol injection [24] (Fig. 2b).

Gadobutrol and related gadolinium tracers were administered to the subarachnoid spaces in mice and rats to disclose the CSF flow through the lymphatics or along the nerve sheaths to extracranial drainage sites, mostly in the cervical lymph nodes. The size of these MRI tracers was around 600 Da, mimicking the metabolites but not the toxic solute proteins. They redistributed from the injection site through the subarachnoid spaces to the paravascular spaces in rodents [49] and even to lateral ventricles. Both in humans [22, 39] and in rodents [53], intrathecally injected MRI tracers were found in deep cervical lymph nodes after minutes to hours.

The difference of the extent of the redistribution in the subarachnoid/paravascular CSF spaces was examined during sleep, awake states, and under anesthesia (Fig. 6b) using fluorescent dyes and under anesthesia also using MRI [49, 53]. Though there are contradictory results in the literature, a consensus has been reached that Gd-tracer CSF MRI studies reveal (1) glymphatic flow from ISF to subarachnoid CSF are enhanced during sleep (especially NREM sleep) and thus CSF MRI tracers redistribute only to the subarachnoid spaces and least to the paravascular spaces [66] and (2) earlier studies of CSF influx (increased redistribution to the paravascular spaces) should now be interpreted cautiously regarding whether the glymphatic flow was affected by the drop of intracranial pressure associated with intra-cisterna (magna) puncture [54, 55, 57] (Fig. 6d) and/or anesthesia effect [18, 67] (Fig. 6a, b). Various anesthetic agents and their effect on glymphatic flow were reported for their impact on the glymphatic flow [67] and probably associated functional connectivity [133].

As glymphatic flow is influenced by the experimental scheme, MRI studies should also be cautiously interpreted. Intrathecal injection and later acquisition make the findings reliable and robust, meaning high reproducibility. And interestingly, this least invasive technique has been popularly used traditionally in RI cisternography in humans. Intra-cisterna injection and examining acute changes on glymphatic flow using fluorescent dyes might have not revealed the real physiological long-term basal status of, for example, dementia subjects and thus the effect of pharmacological intervention. This would have taken place even though investigators used MRI CSF tracers. Anesthesia and sleep do not seem to share their effect on the glymphatic flow [54]. This is because sleep increases ISF efflux and CSF-lymphatic drainage [66] and that anesthesia (isoflurane as an example) blocks ISF efflux and thus CSR-lymphatic outflow [53]. Among many anesthetic agents, the light concentration of isoflurane and dexmedetomidine (alpha-2 agonist) and probably ketamine/xylazine mimics most of the sleep state [55].

On MRI studies in humans, investigators looked for evidence that CSF is drained via cribriform plates/nasal routes, but there is no evidence yet (Fig. 9). Currently, we think that in humans, CSF is mainly drained to dorsal dural meningeal lymphatics, which travel through deep lymphatics of the head, face, and neck to the deep cervical lymph nodes. Even though nasal pathways with olfactory nerves are used, it would be no more than optic, facial, or other cranial nerve sheaths in humans.

MRI imaging of the CSF suggested that CSF flow is compartmentalized [44] (Fig. 4c). According to the vector flow images (time-resolved 3D phase-contrast image) of lateral ventricles (frontal/occipital and temporal horns) and the third/fourth ventricles, CSF produced from choroid plexus are mixed and circulate in a complex manner probably to exchange interstitial solutes with CSF through ependymal gap junctions [8] and then even showed to-and-fro movement through aqueduct connecting third and fourth ventricles [46] (Fig. 4d). This meant that this flow is maintaining the patency of aqueduct which has a small caliber especially in smaller animals like mice [46]. In humans when there is an obstruction of cisterns and thus obstructive hydrocephalus, this is the natural buildup of ventricular reflux from subarachnoid space [41]. Since long ago, this ventricular reflux was considered to function to mitigate the increased intracranial pressure and supplied

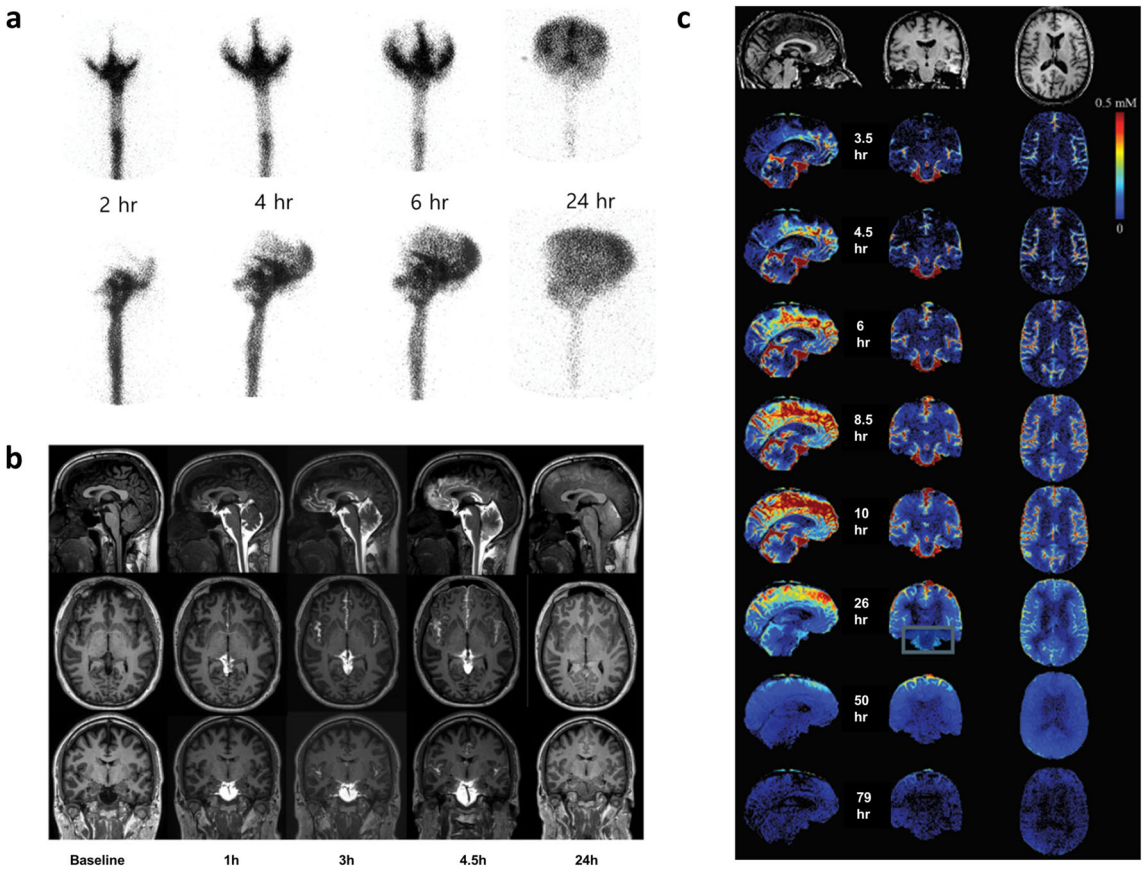

Fig. 9 Intrathecal contrast MRI and radioisotope (RI) cisternography. **a** Classic example of RI cisternography shows that after intrathecal injection, basal cistern appears at 2 h; at 4 h, interhemispheric and Sylvian fissures are well visualized. At 24 h, the entire silhouette of both hemispheres is seen. What we did not know is that on the 24-h image, Tc-99m DTPA stayed not only in subarachnoid spaces but also in paravascular spaces and that remaining Tc-99m DTPA had been or would have been absorbed not by arachnoid villi but more likely across arachnoid barrier layer to parasagittal dura and to the meningeal lymphatics to reach deep cervical lymph nodes. Reprinted with permission from Koh [41]. **b** After intrathecal gadobutrol injection, 24-h delay image was taken showing the disappearance of basal cisternal gadobutrol in a normal subject. Abnormal findings were observed that gadobutrol stayed in the subarachnoid space over the hemispheres and cisterns and also ventricular refluxes. Reprinted with permission from Ringstad et al. [134]. **c** After intrathecal gadobutrol injection in normal volunteer, a 79-h image was taken to reveal that the gadobutrol has almost completely disappeared. Reprinted with permission from Watts et al. [51]

the indication of ventriculo-peritoneal shunt operation in these hydrocephalus patients with ventricular reflux on RI cisternography [41].

Spinal CSF was also proposed to be cleared on-site despite gross global flow [32]. This means that CSF in the subarachnoid space flows over the spinal cord and from the head to the lumbosacral areas via over the cords or through the spinal canal. Along with this gross flow, CSF is also using spinal meningeal lymphatic vessels to be drained to the systemic circulation [32, 34]. The relative contribution of this route over the global brain/spinal cord drainage is yet to be found. In the cervical spinal cord, spinal meningeal lymphatic vessels drain CSF through spinal nerve outlets to the cervical lymph nodes too [33]. This means that deep cervical lymph nodes are gathering sink of lymphatics from cranial (via dural meningeal and other neural pathways) [30] and neck (via cervical spinal meningeal) areas [32, 34].

Nuclear and PET Imaging Studies Trying to Elucidate Glymphatic and Lymphatic Flow

RI cisternography can be used easily for imaging glymphatic flow in a longer timeframe with a smaller amount of chemical, mostly In-111 DTPA [41]. When using In-111 with DTPA, we use Ca^{2+} protection method of unlabeled DTPA to reduce the risk of possible side effects of chelating Ca^{2+} in the CSF (and the spinal cord in the vicinity). Tc-99m DTPA has been and is used for RI cisternography too, but in this case, one should be so cautious that the unlabeled DTPA should be saturated by Tc-99 DTPA or Tc-99m DTPA [41]. Traditionally, we did not acquire the images after 24 h and the 24-h image was not examined in detail for any sign of functioning or dysfunctional CSF-lymphatic flow (Fig. 9b). When referring to MRI studies using Gd DTPA, deep cervical lymph nodes may be imaged to assess or quantify the amount

of CSF-lymphatic flow to the extracranial lymphatics by RI cisternography [39]. This amount can be used to quantify the drained amount even to unravel the contribution of head and cervical spine meningeal lymphatics to the clearance of CSF and their toxic solutes such as amyloid oligomer and extracellular tau.

Recently, there showed up two papers in a journal groping, the possibility of using amyloid plaque and tau neurofibrillary tangle imaging PET (C-11 PIB and F-18 THK5117) for further glymphatic-lymphatic outflow study and quantitative analysis. One report [61] used dynamic PET images of F-18 THK5117, and by estimating the correlation of time-activity curves between ventricular CSF and extracranial voxel, the CSF-positive extracranial voxels are identified to be highly detected in the nasal cavity. Another study [62] used a different approach but their assumption was also the same as they tried to elucidate the nasal route by compartmental analysis of clearance of lateral ventricular C-11 activity. This study was neutral in interpretation while not maintaining clearance through the cribriform plate for the reduced clearance of C-11 PIB from the lateral ventricle (and thus CSF). In a recent MRI study [51] at a long term of 96 h after intrathecal injection of gadobutrol in human healthy subjects, there were no nasal cavity activities (Fig. 9c). Furthermore, other MRI studies [24, 39, 134] reported strong evidence that the nasal route is not used in humans. As a result, by any chance, if humans do not use this route and at most, just a little fraction is drained via nasal cavity unlike small animals, this study would have pursued an artifact [24, 39, 134] while trying to discover the author's preset belief that the radioactivity of nasal mucosa might reveal the drainage of CSF via the cribriform plate. Thus, the above preliminary PET studies should further be validated. Still, to elucidate the efflux of CSF through any routes including meningeal lymphatics, perineural, or others, intrathecally administered radionuclide-labeled radiopharmaceuticals would be the best choice, considering the weak contrast of gadobutrol.

Conclusion

Based on the understanding regarding how the brain glymphatic/lymphatics contribute to the waste drainage from ISF-CSF via lymphatic pathways, elucidated in rodents and in humans, MRI and PET imaging can help evaluate the function and dysfunction of glymphatic and lymphatics in various pathological states. Sleep-wake status, anesthesia, and physiologic or neurodegenerative disease-related consequences on glymphatic and lymphatics are now to be interpreted properly in humans using intrathecal contrast-enhanced MRI and PET.

Funding This research was supported by the National Research Foundation of Korea (NRF) grant funded by the Korean Government (MSIP) (No. 2015M3C7A1028926 and No. 2017M3C7A1048079) and NRF grant funded by the Korean Government (No. 2016R1D1A1A02937497 and No. 2017R1A5A1015626).

Compliance with Ethical Standards

Conflict of Interest Dong Soo Lee, Minseok Suh, Azmal Sarker, and Yoori Choi declare that they have no conflict of interest.

Ethical Approval All procedures performed in studies were in accordance with the ethical standards of the institutional and/or national research committee and with the 1964 Helsinki declaration and its later amendments or comparable ethical standards.

Informed Consent As a review article, obtaining informed consent was waived.

References

1. Iliff JJ, Wang M, Liao Y, Plogg BA, Peng W, Gundersen GA, et al. A paravascular pathway facilitates CSF flow through the brain parenchyma and the clearance of interstitial solutes, including amyloid. β Sci Transl Med. 2012;4:147ra111.
2. Louveau A, Smirnov I, Keyes TJ, Eccles JD, Rouhani SJ, Peske JD, et al. Structural and functional features of central nervous system lymphatic vessels. Nature. 2015;523:337–41.
3. Iliff JJ, Wang M, Zeppenfeld DM, Venkataraman A, Plog BA, Liao Y, et al. Cerebral arterial pulsation drives paravascular CSF-interstitial fluid exchange in the murine brain. J Neurosci. 2013;33:18190–9.
4. Aspelund A, Antila S, Proulx ST, Karlsen TV, Karaman S, Detmar M, et al. A dural lymphatic vascular system that drains brain interstitial fluid and macromolecules. J Exp Med. 2015;212:991–9.
5. Smith AJ, Yao X, Dix JA, Jin BJ, Verkman AS. Test of the 'glymphatic' hypothesis demonstrates diffusive and aquaporin-4-independent solute transport in rodent brain parenchyma. Elife. 2017;6:e27679.
6. Lei Y, Han H, Yuan F, Javeed A, Zhao Y. The brain interstitial system: anatomy, modeling, in vivo measurement, and applications. Prog Neurobiol. 2017;157:230–46.
7. Mestre H, Hablitz LM, Xavier ALR, Feng W, Zou W, Pu T, et al. Aquaporin-4-dependent glymphatic solute transport in the rodent brain. Elife. 2018;7:e40070.
8. Nakada T, Kwee IL. Fluid dynamics inside the brain barrier: current concept of interstitial flow, glymphatic flow, and cerebrospinal fluid circulation in the brain. Neuroscientist. 2019;25:155–66.
9. Iliff J, Simon M. CrossTalk proposal: the glymphatic system supports convective exchange of cerebrospinal fluid and brain interstitial fluid that is mediated by perivascular aquaporin-4. J Physiol. 2019;597:4417–9.
10. Smith AJ, Verkman AS. CrossTalk opposing view: going against the flow: interstitial solute transport in brain is diffusive and aquaporin-4 independent. J Physiol. 2019;597:4421–4.
11. Smith AJ, Verkman AS. Rebuttal from Alex J. Smith and Alan S. Verkman. J Physiol. 2019;597:4427–8.
12. Louveau A, Plog BA, Antila S, Alitalo K, Nedergaard M, Kipnis J. Understanding the functions and relationships of the glymphatic system and meningeal lymphatics. J Clin Invest. 2017;127:3210–9.

13. Raper D, Louveau A, Kipnis J. How do meningeal lymphatic vessels drain the CNS? Trends Neurosci. 2016;39:581–6.
14. Antila S, Karaman S, Nurmi H, Airavaara M, Voutilainen MH, Mathivet T, et al. Development and plasticity of meningeal lymphatic vessels. J Exp Med. 2017;214:3645–67.
15. Da Mesquita S, Louveau A, Vaccari A, Smirnov I, Cornelison RC, Kingsmore KM, et al. Functional aspects of meningeal lymphatics in ageing and Alzheimer's disease. Nature. 2018;560:185–91.
16. Frederick N, Louveau A. Meningeal lymphatics, immunity and neuroinflammation. Curr Opin Neurobiol. 2020;62:41–7.
17. Da Mesquita S, Fu Z, Kipnis J. The meningeal lymphatic system: a new player in neurophysiology. Neuron. 2018;100:375–88.
18. Xie L, Kang H, Xu Q, Chen MJ, Liao Y, Thiyagarajan M, et al. Sleep drives metabolite clearance from the adult brain. Science (80-). 2013;342:373–7.
19. Kress BT, Iliff JJ, Xia M, Wang M, Wei HS, Zeppenfeld D, et al. Impairment of paravascular clearance pathways in the aging brain. Ann Neurol. 2014;76:845–61.
20. Mastorakos P, McGavern D. The anatomy and immunology of vasculature in the central nervous system. Sci Immunol 2019;4: eaav0492.
21. Coles JA, Myburgh E, Brewer JM, McMenamin PG. Where are we? The anatomy of the murine cortical meninges revisited for intravital imaging, immunology, and clearance of waste from the brain. Prog Neurobiol. 2017;156:107–48.
22. Zhou Y, Cai J, Zhang W, Gong X, Yan S, Zhang K, et al. Impairment of the glymphatic pathway and putative meningeal lymphatic vessels in the aging human. Ann Neurol. 2020;87: 357–69.
23. Castro Dias M, Mapunda JA, Vladymyrov M, Engelhardt B. Structure and junctional complexes of endothelial, epithelial and glial brain barriers. Int J Mol Sci. 2019;20:5372.
24. Ringstad G, Eide PK. Cerebrospinal fluid tracer efflux to parasagittal dura in humans. Nat Commun. 2020;11:1–9.
25. Goodman JR, Adham ZO, Woltjer RL, Lund AW, Iliff JJ. Characterization of dural sinus-associated lymphatic vasculature in human Alzheimer's dementia subjects. Brain Behav Immun. 2018;73:34–40.
26. Dupont G, Schmidt C, Yilmaz E, Oskouian RJ, Macchi V, de Caro R, et al. Our current understanding of the lymphatics of the brain and spinal cord. Clin Anat. 2019;32:117–21.
27. Ahn JH, Cho H, Kim JH, Kim SH, Ham JS, Park I, et al. Meningeal lymphatic vessels at the skull base drain cerebrospinal fluid. Nature. 2019;572:62–6.
28. Lüdemann W, von Rautenfeld DB, Samii M, Brinker T. Ultrastructure of the cerebrospinal fluid outflow along the optic nerve into the lymphatic system. Childs Nerv Syst. 2005;21:96–103.
29. Walter BA, Valera VA, Takahashi S, Ushiki T. The olfactory route for cerebrospinal fluid drainage into the peripheral lymphatic system. Neuropathol Appl Neurobiol. 2006;32:388–96.
30. Ma Q, Ineichen BV, Detmar M, Proulx ST. Outflow of cerebrospinal fluid is predominantly through lymphatic vessels and is reduced in aged mice. Nat Commun. 2017;8:1434.
31. Wang X, Lou N, Eberhardt A, Yang Y, Kusk P, Xu Q, et al. An ocular glymphatic clearance system removes β-amyloid from the rodent eye. Sci Transl Med. 2020;12:eaaw3210.
32. Miura M, Kato S, Von Lüdinghausen M. Lymphatic drainage of the cerebrospinal fluid from monkey spinal meninges with special reference to the distribution of the epidural lymphatics. Arch Histol Cytol. 1998;61:277–86.
33. Clapham R, O'sullivan E, Weller RO, Carare RO. Cervical lymph nodes are found in direct relationship with the internal carotid artery: significance for the lymphatic drainage of the brain. Clin Anat 2009;23:43–47.
34. Jacob L, Boisserand LSB, Geraldo LHM, de Brito Neto J, Mathivet T, Antila S, et al. Anatomy and function of the vertebral column lymphatic network in mice. Nat Commun. 2019;10:4594.
35. Kuo PH, Stuehm C, Squire S, Johnson K. Meningeal lymphatic vessel flow runs countercurrent to venous flow in the superior sagittal sinus of the human brain. Tomography. 2018;4:99–104.
36. Maloveska M, Danko J, Petrovova E, Kresakova L, Vdoviakova K, Michalicova A, et al. Dynamics of Evans blue clearance from cerebrospinal fluid into meningeal lymphatic vessels and deep cervical lymph nodes. Neurol Res. 2018;40:372–80.
37. Bradbury MW, Cole DF. The role of the lymphatic system in drainage of cerebrospinal fluid and aqueous humour. J Physiol. 1980;299:353–65.
38. Boulton M, Flessner M, Armstrong D, Hay J, Johnston M. Determination of volumetric cerebrospinal fluid absorption into extracranial lymphatics in sheep. Am J Physiol - Regul Integr Comp Physiol. 1998;274:R88–96.
39. Eide PK, Vatnehol SAS, Emblem KE, Ringstad G. Magnetic resonance imaging provides evidence of glymphatic drainage from human brain to cervical lymph nodes. Sci Rep. 2018;8:7194.
40. Ma Q, Ries M, Decker Y, Müller A, Riner C, Bücker A, et al. Rapid lymphatic efflux limits cerebrospinal fluid flow to the brain. Acta Neuropathol. 2019;137:151–65.
41. Koh Chang-Soon Nuclear Medicine. Korea; 2008.
42. Grubb S, Lauritzen M. Deep sleep drives brain fluid oscillations. Science. 2019;366:572–3.
43. Iadecola C. The neurovascular unit coming of age: a journey through neurovascular coupling in health and disease. Neuron. 2017;96:17–42.
44. Matsumae M, Kuroda K, Yatsushiro S, Hirayama A, Hayashi N, Takizawa K, et al. Changing the currently held concept of cerebrospinal fluid dynamics based on shared findings of cerebrospinal fluid motion in the cranial cavity using various types of magnetic resonance imaging techniques. Neurol Med Chir (Tokyo). 2019;59:133–46.
45. Hirayama A, Matsumae M, Yatsushiro S, Abdulla A, Atsumi H, Kuroda K. Visualization of pulsatile CSF motion around membrane-like structures with both 4D velocity mapping and time-SLIP technique. Magn Reson Med Sci. 2015;14:263–73.
46. Fultz NE, Bonmassar G, Setsompop K, Stickgold RA, Rosen BR, Polimeni JR, et al. Coupled electrophysiological, hemodynamic, and cerebrospinal fluid oscillations in human sleep. Science (80-). 2019;366:628–31.
47. Matsumae M, Hirayama A, Atsumi H, Yatsushiro S, Kuroda K. Velocity and pressure gradients of cerebrospinal fluid assessed with magnetic resonance imaging-clinical article. J Neurosurg. 2014;120:218–27.
48. Murtha LA, Yang Q, Parsons MW, Levi CR, Beard DJ, Spratt NJ, et al. Cerebrospinal fluid is drained primarily via the spinal canal and olfactory route in young and aged spontaneously hypertensive rats. Fluids Barriers CNS. 2014;11:12.
49. Iliff JJ, Lee H, Yu M, Feng T, Logan J, Nedergaard M, et al. Brain-wide pathway for waste clearance captured by contrast-enhanced MRI. J Clin Invest. 2013;123:1299–309.
50. Absinta M, Ha SK, Nair G, Sati P, Luciano NJ, Palisoc M, et al. Human and nonhuman primate meninges harbor lymphatic vessels that can be visualized noninvasively by MRI. Elife. 2017;6: e29738.
51. Watts R, Steinklein JM, Waldman L, Zhou X, Filippi CG. Measuring glymphatic flow in man using quantitative contrast-enhanced MRI. Am J Neuroradiol. 2019;40:648–51.
52. Suzuki K, Yamada K, Nakada K, Suzuki Y, Watanabe M, Kwee IL, et al. MRI characteristics of the glia limitans externa: a 7T study. Magn Reson Imaging. 2017;44:140–5.

53. Gakuba C, Gaberel T, Goursaud S, Bourges J, D Palma C, Quenault A, et al. General anesthesia inhibits the activity of the "glymphatic system" Theranostics 2018;8:710–722.
54. Benveniste H, Heerdt PM, Fontes M, Rothman DL, Volkow ND. Glymphatic system function in relation to anesthesia and sleep states. Anesth Analg. 2019;128:747–58.
55. Benveniste H, Lee H, Ding F, Sun Q, Al-Bizri E, Makaryus R, et al. Anesthesia with dexmedetomidine and low-dose isoflurane increases solute transport via the glymphatic pathway in rat brain when compared with high-dose isoflurane. Anesthesiology. 2017;127:976–88.
56. Benveniste H, Liu X, Koundal S, Sanggaard S, Lee H, Wardlaw J. The Glymphatic system and waste clearance with brain aging: a review. Gerontology. 2019;65:106–19.
57. Lundgaard I, Lu ML, Yang E, Peng W, Mestre H, Hitomi E, et al. Glymphatic clearance controls state-dependent changes in brain lactate concentration. J Cereb Blood Flow Metab. 2017;37:2112–24.
58. Lundgaard I, Wang W, Eberhardt A, Vinitsky HS, Reeves BC, Peng S, et al. Beneficial effects of low alcohol exposure, but adverse effects of high alcohol intake on glymphatic function. Sci Rep 2018;8:2246.
59. Taoka T, Jost G, Frenzel T, Naganawa S, Pietsch H. Impact of the glymphatic system on the kinetic and distribution of gadodiamide in the rat brain. Investig Radiol. 2018;53:529–34.
60. Taoka T, Naganawa S. Glymphatic imaging using MRI. J Magn Reson Imaging. 2020;51:11–24.
61. De Leon MJ, Li Y, Okamura N, Tsui WH, Saint-Louis LA, Glodzik L, et al. Cerebrospinal fluid clearance in Alzheimer disease measured with dynamic PET. J Nucl Med. 2017;58:1471–6.
62. Schubert JJ, Veronese M, Marchitelli L, Bodini B, Tonietto M, Stankoff B, et al. Dynamic 11C-PIB PET shows cerebrospinal fluid flow alterations in Alzheimer disease and multiple sclerosis. J Nucl Med. 2019;60:1452–60.
63. Smith AJ, Verkman AS. The "glymphatic" mechanism for solute clearance in Alzheimer's disease: game changer or unproven speculation? FASEB J. 2018;32:543–51.
64. Asgari M, De Zélicourt D, Kurtcuoglu V. Glymphatic solute transport does not require bulk flow. Sci Rep. 2016;6:38635.
65. Kounda S, Elkin R, Nadeem S, Xue Y, Constantinou S, Sanggaard S, et al. Optimal mass transport with Lagrangian workflow reveals advective and diffusion driven solute transport in the glymphatic system. Sci Rep 2020;10:1990.
66. Cai X, Qiao J, Kulkarni P, Harding IC, Ebong E, Ferris CF. Imaging the effect of the circadian light–dark cycle on the glymphatic system in awake rats. Proc Natl Acad Sci U S A. 2020;117:668–76.
67. Hablitz LM, Vinitsky HS, Sun Q, Stæger FF, Sigurdsson B, Mortensen KN, et al. Increased glymphatic influx is correlated with high EEG delta power and low heart rate in mice under anesthesia. Sci Adv. 2019;5:eaav5447.
68. Achariyar TM, Li B, Peng W, Verghese PB, Shi Y, McConnell E, et al. Glymphatic distribution of CSF-derived apoE into brain is isoform specific and suppressed during sleep deprivation. Mol Neurodegener 2016;11:74.
69. DiNuzzo M, Nedergaard M. Brain energetics during the sleep–wake cycle. Curr Opin Neurobiol. 2017;47:65–72.
70. Gandhi GK, Cruz NF, Ball KK, Dienel GA. Astrocytes are poised for lactate trafficking and release from activated brain and for supply of glucose to neurons. J Neurochem. 2009;111:522–36.
71. Verkhratsky A, Nedergaard M. Physiology of astroglia. Physiol Rev. 2018;98:239–389.
72. Brown RE, Basheer R, McKenna JT, Strecker RE, McCarley RW. Control of sleep and wakefulness. Physiol Rev. 2012;92:1087–187.
73. Cordone S, Annarumma L, Rossini PM, De Gennaro L. Sleep and β-amyloid deposition in Alzheimer disease: insights on mechanisms and possible innovative treatments. Front Pharmacol 2019;10:659.
74. Ooms S, Overeem S, Besse K, Rikkert MO, Verbeek M, Claassen JAHR. Effect of 1 night of total sleep deprivation on cerebrospinal fluid β-amyloid 42 in healthy middle-aged men a randomized clinical trial. JAMA Neurol. 2014;71:971–7.
75. Shokri-Kojori E, Wang GJ, Wiers CE, Demiral SB, Guo M, Kim SW, et al. β-Amyloid accumulation in the human brain after one night of sleep deprivation. Proc Natl Acad Sci U S A. 2018;115:4483–8.
76. Leenaars CHC, Savelyev SA, Van der Mierden S, Joosten RNJMA, Dematteis M, Porkka-Heiskanen T, et al. Intracerebral adenosine during sleep deprivation: a meta-analysis and new experimental data. J Circadian Rhythms. 2018;16:1–11.
77. Kang JE, Lim MM, Bateman RJ, Lee JJ, Smyth LP, Cirrito JR, et al. Amyloid-β dynamics are regulated by orexin and the sleep-wake cycle. Science. 2009;326(80):1005–7.
78. Holth JK, Fritschi SK, Wang C, Pedersen NP, Cirrito JR, Mahan TE, et al. The sleep-wake cycle regulates brain interstitial fluid tau in mice and CSF tau in humans. Science. 2019;363(80):80–884.
79. Noble W, Spires-Jones TL. Sleep well to slow Alzheimer's progression? Sleep disruption promotes the spread of damaging tau pathology in Alzheimer's disease. Science. 2019;363(80):813–4.
80. Papadopoulos MC, Verkman AS. Aquaporin water channels in the nervous system. Nat Rev Neurosci. 2013;14:265–77.
81. Haydon PG. Astrocytes and the modulation of sleep. Curr Opin Neurobiol. 2017;44:28–33.
82. Ribeiro-Rodrigues TM, Martins-Marques T, Morel S, Kwak BR, Girão H. Role of connexin 43 in different forms of intercellular communication-gap junctions, extracellular vesicles and tunnelling nanotubes. J Cell Sci. 2017;130:3619–30.
83. Azevedo FAC, Carvalho LRB, Grinberg LT, Farfel JM, Ferretti REL, Leite REP, et al. Equal numbers of neuronal and nonneuronal cells make the human brain an isometrically scaled-up primate brain. J Comp Neurol. 2009;513:532–41.
84. von Bartheld CS, Bahney J, Herculano-Houzel S. The search for true numbers of neurons and glial cells in the human brain: a review of 150 years of cell counting. J Comp Neurol. 2016;524:3865–95.
85. Triacca V, Güç E, Kilarski WW, Pisano M, Swartz MA. Transcellular pathways in lymphatic endothelial cells regulate changes in solute transport by fluid stress. Circ Res. 2017;120:1440–52.
86. Berridge CW, Schmeichel BE, España RA. Noradrenergic modulation of wakefulness/arousal. Sleep Med Rev. 2012;16:187–97.
87. Greene RW, Bjorness TE, Suzuki A. The adenosine-mediated, neuronal-glial, homeostatic sleep response. Curr Opin Neurobiol. 2017;44:236–42.
88. Hauglund NL, Pavan C, Nedergaard M. Cleaning the sleeping brain–the potential restorative function of the glymphatic system. Curr Opin Physiol. 2020;15:1–6.
89. Ries M, Sastre M. Mechanisms of Aβ clearance and degradation by glial cells. Front Aging Neurosci. 2016;8:160.
90. Zuroff L, Daley D, Black KL, Koronyo-Hamaoui M. Clearance of cerebral Aβ in Alzheimer's disease: reassessing the role of microglia and monocytes. Cell Mol Life Sci. 2017;74:2167–201.
91. Yamazaki Y, Zhao N, Caulfield TR, Liu CC, Bu G. Apolipoprotein E and Alzheimer disease: pathobiology and targeting strategies. Nat Rev Neurol. 2019;15:501–18.
92. Shi Y, Holtzman DM. Interplay between innate immunity and Alzheimer disease: APOE and TREM2 in the spotlight. Nat Rev Immunol. 2018;18:759–72.
93. Yeh FL, Hansen DV, Sheng M. TREM2, microglia, and neurodegenerative diseases. Trends Mol Med. 2017;23:512–33.
94. Hansen DV, Hanson JE, Sheng M. Microglia in Alzheimer's disease. J Cell Biol. 2018;217:459–72.

95. Mathys H, Davila-Velderrain J, Peng Z, Gao F, Mohammadi S, Young JZ, et al. Single-cell transcriptomic analysis of Alzheimer's disease. Nature. 2019;570:332–7.
96. Guo JL, Lee VMY. Cell-to-cell transmission of pathogenic proteins in neurodegenerative diseases. Nat Med. 2014;20:130–8.
97. Peng C, Trojanowski JQ, Lee VMY. Protein transmission in neurodegenerative disease. Nat Rev Neurol. 2020;16:199–212.
98. Vaquer-Alicea J, Diamond MI. Propagation of protein aggregation in neurodegenerative diseases. Annu Rev Biochem. 2019;88:785–810.
99. Chen XQ, Mobley WC. Alzheimer disease pathogenesis: insights from molecular and cellular biology studies of oligomeric Aβ and tau species. Front Neurosci 2019;13:659.
100. Canter RG, Penney J, Tsai LH. The road to restoring neural circuits for the treatment of Alzheimer's disease. Nature. 2016;539:187–96.
101. Španić E, Langer Horvat L, Hof PR, Šimić G. Role of microglial cells in Alzheimer's disease tau propagation. Front Aging Neurosci. 2019;11:271.
102. Liddelow SA, Guttenplan KA, Clarke LE, Bennett FC, Bohlen CJ, Schirmer L, et al. Neurotoxic reactive astrocytes are induced by activated microglia. Nature. 2017;541:481–7.
103. Rothhammer V, Borucki DM, Tjon EC, Takenaka MC, Chao CC, Ardura-Fabregat A, et al. Microglial control of astrocytes in response to microbial metabolites. Nature. 2018;557:724–8.
104. Zott B, Simon MM, Hong W, Unger F, Chen-Engerer HJ, Frosch MP, et al. A vicious cycle of β amyloid–dependent neuronal hyperactivation. Science. 2019;365(80):559–65.
105. Busche MA, Wegmann S, Dujardin S, Commins C, Schiantarelli J, Klickstein N, et al. Tau impairs neural circuits, dominating amyloid-β effects, in Alzheimer models in vivo. Nat Neurosci. 2019;22:57–64.
106. Götz J, Bodea LG, Goedert M. Rodent models for Alzheimer disease. Nat Rev Neurosci. 2018;19:583–98.
107. van der Kant R, Goldstein LSB, Ossenkoppele R. Amyloid-β-independent regulators of tau pathology in Alzheimer disease. Nat Rev Neurosci. 2020;21:21–35.
108. Hardy J, De Strooper B. Alzheimer's disease: where next for anti-amyloid therapies? Brain. 2017;140:853–5.
109. Gauthier S, Alam J, Fillit H, Iwatsubo T, Liu-Seifert H, Sabbagh M, et al. Combination therapy for Alzheimer's disease: perspectives of the EU/US CTAD Task Force. J Prev Alzheimer's Dis. 2019;6:164–8.
110. Vander Zanden CM, Chi EY. Passive immunotherapies targeting amyloid beta and tau oligomers in Alzheimer's disease. J Pharm Sci. 2020;109:68–73.
111. Liu CC, Hu J, Zhao N, Wang J, Wang N, Cirrito JR, et al. Astrocytic LRP1 mediates brain Aβ clearance and impacts amyloid deposition. J Neurosci. 2017;37:4023–31.
112. Lee Y, Choi Y, Park E-J, Kwon S, Kim H, Lee JY, et al. Improvement of glymphatic-lymphatic drainage of beta-amyloid by focused ultrasound in Alzheimer's disease model. bioRxiv 2020; Sci Rep in revision.
113. Patel TK, Habimana-Griffin L, Gao X, Xu B, Achilefu S, Alitalo K, et al. Dural lymphatics regulate clearance of extracellular tau from the CNS. Mol Neurodegener. 2019;14:11.
114. Dupont G, Iwanaga J, Yilmaz E, Tubbs RS. Connections between amyloid beta and the meningeal lymphatics as a possible route for clearance and therapeutics. Lymphat Res Biol. 2020;18:2–6.
115. Louveau A, Da Mesquita S, Kipnis J. Lymphatics in neurological disorders: a neuro-Lympho-vascular component of multiple sclerosis and Alzheimer's disease? Neuron. 2016;91:957–73.
116. Romanova L, Philips H, Calip G, Hauser K, Peterson D, Lazarov O, et al. Energy-dependent transport at dural lymphatic vessels is necessary for Aβ brain clearance in Alzheimer's disease. bioRxiv. 2019;427617.
117. Yoffey JM, Drinker CK. The lymphatic pathway from the nose and pharynx: the absorption of dyes. J Exp Med. 1938;68:1–12.
118. Larsen S, Landolt H, Berger W, Nedergaard M, Knudsen G, Holst S. Haplotype of the astrocytic water channel AQP4 modulates slow wave energy in human NREM sleep. PLoS Biology. 2020;18.5:e3000623.
119. Jordão JF, Thévenot E, Markham-Coultes K, Scarcelli T, Weng YQ, Xhima K, et al. Amyloid-β plaque reduction, endogenous antibody delivery and glial activation by brain-targeted, transcranial focused ultrasound. Exp Neurol. 2013;248:16–29.
120. Burgess A, Dubey S, Yeung S, Hough O, Eterman N, Aubert I, et al. Alzheimer disease in a mouse model: Mr imaging-guided focused ultrasound targeted to the hippocampus opens the blood-brain barrier and improves pathologic abnormalities and behavior. Radiology. 2014;273:736–45.
121. Leinenga G, Götz J. Scanning ultrasound removes amyloid-b and restores memory in an Alzheimer's disease mouse model. Sci Transl Med. 2015;7. 278:278ra33-278ra33.
122. Poon CT, Shah K, Lin C, Tse R, Kim KK, Mooney S, et al. Time course of focused ultrasound effects on β-amyloid plaque pathology in the TgCRND8 mouse model of Alzheimer's disease. Sci Rep. 2018;8:1–11.
123. Karakatsani ME, Kugelman T, Ji R, Murillo M, Wang S, Niimi Y, et al. Unilateral focused ultrasound-induced blood-brain barrier opening reduces phosphorylated tau from the rTg4510 mouse model. Theranostics. 2019;9:5396–411.
124. Pandit R, Leinenga G, Götz J. Repeated ultrasound treatment of tau transgenic mice clears neuronal tau by autophagy and improves behavioral functions. Theranostics. 2019;9:3754–67.
125. Meng Y, Abrahao A, Heyn CC, Bethune AJ, Huang Y, Pople CB, et al. Glymphatics visualization after focused ultrasound-induced blood–brain barrier opening in humans. Ann Neurol. 2019;86:975–80.
126. xu LD, He X, Wu D, Zhang Q, Yang C, yin LF, et al. Continuous theta burst stimulation facilitates the clearance efficiency of the glymphatic pathway in a mouse model of sleep deprivation. Neurosci Lett. 2017;653:189–94.
127. Zeppenfeld DM, Simon M, Haswell JD, D'Abreo D, Murchison C, Quinn JF, et al. Association of perivascular localization of aquaporin-4 with cognition and Alzheimer disease in aging brains. JAMA Neurol. 2017;74:91–9.
128. Gate D, Saligrama N, Leventhal O, Yang AC, Unger MS, Middeldorp J, et al. Clonally expanded CD8 T cells patrol the cerebrospinal fluid in Alzheimer's disease. Nature. 2020;577:399–404.
129. Pan WR, Suami H, Taylor GI. Lymphatic drainage of the superficial tissues of the head and neck: anatomical study and clinical implications. Plast Reconstr Surg. 2008;121:1614–24.
130. Tilney NL. Patterns of lymphatic drainage in the adult laboratory rat. J Anat. 1971;109:369–83.
131. Sakka L, Coll G, Chazal J. Anatomy and physiology of cerebrospinal fluid. Eur Ann Otorhinolaryngol Head Neck Dis. 2011;128:309–16.
132. Herisson F, Frodermann V, Courties G, Rohde D, Sun Y, Vandoorne K, et al. Direct vascular channels connect skull bone marrow and the brain surface enabling myeloid cell migration. Nat Neurosci. 2018;21:1209–17.
133. Paasonen J, Stenroos P, Salo RA, Kiviniemi V, Gröhn O. Functional connectivity under six anesthesia protocols and the awake condition in rat brain. Neuroimage. 2018;172:9–20.
134. Ringstad G, Vatnehol SAS, Eide PK. Glymphatic MRI in idiopathic normal pressure hydrocephalus. Brain. 2017;140:2691–705.